Pyclen-Based Ligands Bearing Pendant Picolinate Arms for Gadolinium Complexation

Gwladys Nizou,[†] Enikő Molnár,[‡] Nadège Hamon,[†] Ferenc Krisztián Kálmán,[‡] Olivier Fougère,[§] Olivier Rousseaux,[§] David Esteban Gòmez,[⊥] Carlos Platas-Iglesias,[⊥] Maryline Beyler,*[,†] Gyula Tircsó*[,‡] and Raphaël Tripier*[,†]

[†] Univ. Brest, UMR-CNRS 6521 CEMCA, 6 avenue Victor le Gorgeu, 29238 BREST, France.

[‡] Department of Physical Chemistry, Faculty of Science and Technology, University of Debrecen, Egyetem tér 1, H-4032 Debrecen, Hungary

[§] Groupe Guerbet, Centre de Recherche d'Aulnay-sous-Bois, BP 57400, 95943 Roissy CdG Cedex, France

[⊥] Centro de Investigacións Científicas Avanzadas (CICA) and Departamento de Química, Universidade da Coruña, Campus da Zapateira-Rúa da Fraga 10, 15008 A Coruña, Spain

ABSTRACT: We report the synthesis of two pyclen-based regioisomer ligands (pyclen = 3,6,9,15-tetraazabicyclo[9.3.1]pentadeca-1(15),11,13-triene) functionalized with picolinic acid pendant arms either at positions ***3,9*-pc2pa** (**L5**) or ***3,6*-pc2pa** (**L6**) of the macrocyclic fragment. The ligands were prepared by regiospecific protection of one of the amine nitrogen atom of the macrocycle using Boc and Alloc protecting groups, respectively. The X-ray structure of the Gd(III) complex of **L5** contains trinuclear $[(Gd\mathbf{L5})_3(H_2O)_3]^{3+}$ entities in which the monomeric units are joined by μ_2-η^1:η^1 carboxylate groups. However, the ^{1}H and ^{89}Y NMR spectra of its Y(III) analogue support the formation of monomeric complexes in solution. The Tb(III) complexes are highly luminescent, with emission quantum yields of up to 50% for $[Tb\mathbf{L5}]^+$. The luminescence lifetimes recorded in H_2O and D_2O solutions indicate the presence of a water molecule coordinated to the metal ion, as also evidenced by the ^{1}H relaxivities measured for the Gd(III) analogues. The Gd(III) complexes present very different exchange rates of the coordinated water molecule (k_{ex}^{298} = 87.1 and 1.06 $\times 10^6$ s^{-1} for $[Gd\mathbf{L5}]^+$ and $[Gd\mathbf{L6}]^+$, respectively). The very high water exchange rate of $[Gd\mathbf{L5}]^+$ is associated to the steric hindrance originated by the coordination of the ligand around the water binding site, which favors a dissociatively activated water exchange process. The Gd(III) complexes present rather high thermodynamic stabilities ($\log K_{GdL}$ = 20.47 and 19.77 for $[Gd\mathbf{L5}]^+$ and $[Gd\mathbf{L6}]^+$, respectively). Furthermore, these complexes are remarkably inert with respect to their acid-assisted dissociation, in particular the complex of **L5**.

INTRODUCTION

The coordination chemistry of lanthanide ions [Ln(III)] in aqueous media attracted an increasing attention during the last 25 years due to several important medical and bioanalytical applications of Ln(III) complexes.[1] For instance, some Gd(III) complexes are currently used as contrast agents in medical magnetic resonance imaging (MRI).[2,3] Some Ln(III) complexes are also characterized by their strong luminescence, with narrow emission bands in the visible and/or infrared regions, long luminescence lifetimes and large Stokes shifts.[4] These properties are particularly interesting to develop luminescent probes for bioanalytical or imaging applications, including complexes with efficient biphotonic excitation or up-conversion in aqueous solution.[5,6] Some efforts have been also directed to attain selective complexation of certain Ln(III) ions, as well as to modulate the stability trend observed across the lanthanide series.[7] All these applications require careful ligand design.

The nature of the Ln(III) ions as hard acids within Pearson's classification implies that stable complexation in aqueous solution requires the use of polydentate ligands incorporating hard donor atoms, typically polyamino scaffolds functionalized with carboxylate, phosphonate, phosphinate, amide or hydroxyl groups, to name the most common ones.[8] In particular, the 12-membered macrocyclic structure of cyclen (cyclen = 1,4,7,10-tetraazacyclododecane), functionalized with different pendant arms, often provides highly stable and inert Ln(III) complexes, with the best known ligand of this family being dota (1,4,7,10-tetraazacyclododecane-1,4,7,10-tetraacetic acid, Chart 1).[9]

Chart 1. Chemical structure of the ligands discussed in this work.

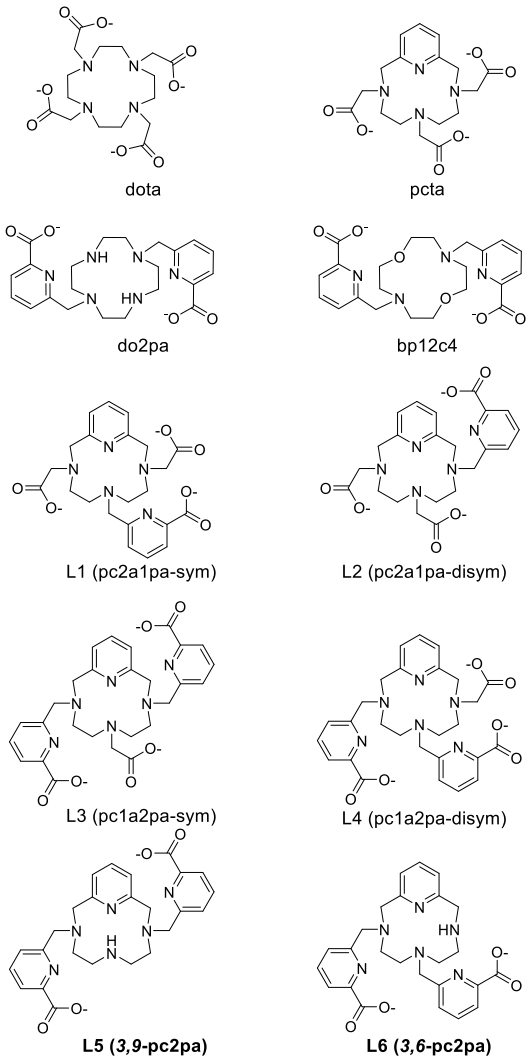

Some years ago, some of us initiated a research program devoted to the design of acyclic and macrocyclic ligands for Ln(III) complexation incorporating picolinate units. Introducing the picolinate motif into different ligand scaffolds is very appealing, as it allows incorporating two donor atoms by functionalization of a single amine nitrogen, leaving N atoms available for further functionalization without decreasing ligand denticity. Different open-chain octadentate ligands were found to form very stable complexes with the Ln(III) ions,[10] though they generally yield fast dissociation kinetics.[11] The lability of the complexes can be alleviated by ligand rigidification, yet macrocyclic ligands often form, in return, more inert complexes.[12] The incorporation of picolinate groups also increase the macrocyclic rigidity and their insertion to crown ethers of different sizes was found to be a very robust approach to enhance the selectivity of the ligand to certain Ln(III) ions.[13] However, even the derivative based on the small 12-membered diaza-12-crown-12 macrocycle (bp12c4, Chart 1) forms rather labile Ln(III) complexes, in spite of their high thermodynamic stability.[14,15] Subsequently, we found the use of cyclen as the macrocyclic motif (i.e. do2pa, Chart 1) yields considerably more inert complexes,[16] whose picolinate units can be optimized for two-photon absorption microscopy.[17]

More recently, we investigated the series of pyclen-based ligands, named here **L1**-**L4** for simplicity (Chart 1), which form very stable Ln(III) complexes, in particular those with the dipicolinate pyclen chelators **L3** and **L4**[18,19] (**pc1a2pa -sym** and -**disym** respectively) that offer 9 donor atoms for coordination to the Ln(III) center.[20] These ligands form more stable Gd(III) complexes than the heptadentate pcta ligand.[19] The picolinate units can be further functionalized to yield highly luminescent Ln(III) probes for one- and two-photon bioimaging applications in vitro and in vivo.[21] Moreover, we proved that the different arrangement of the pendant arms attached to the macrocyclic structure affects significantly the stability constants of the metal complexes. However, the presence of nine coordinating atoms in [Gd**L3**] and [Gd**L4**] did not allow the coordination of water molecule, whereas the substitution of one picolinate by an acetate arm resulted in monohydrated Gd(III) chelates ([Gd**L1**(H_2O)] and [Gd**L2**(H_2O)]) based on **pc2a1pa -sym** and -**disym** respectively, but also provoked a significant decrease of complexes stability.[Erreur ! Signet non défini.,Erreur ! Signet non défini.] Thus, we envisaged to prepare octadentate ligands with improved stability and kinetic inertness by conserving two picolinate moieties attached to the macrocyclic structure, which was achieved with **L5** and **L6** (Chart 1). We present here the synthesis of the two regioisomer ligands and a detailed characterization of the complexes, including their structural features, photophysical properties, thermodynamic stability and dissociation kinetics.

RESULTS AND DISCUSSION

Syntheses of the ligands and complexes. The syntheses of the symmetric and non-symmetric dipicolinate pyclen ligands ***3,9*-pc2pa** (**L5**) or ***3,6*-pc2pa** (**L6**) are depicted in Schemes 1 and 2. The synthesis of the first regioisomer, **L5** (Scheme 1), started from N3-pyclen-Boc (**1**), which was previously reported by Siauge *et al*.[22] As already described,[18a] the two picolinate moieties were introduced on the two secondary amine functions of compound **1** to give the intermediate compound **2** (Figures S1-S2, Supporting Information). To decrease the reaction time, the procedure was slightly modified with the use of NaI and reflux heating. The reaction time efficiently dropped from 6 days to 7 hours, while additionally the yield increased from 63% to 95%. Removal of the protecting Boc group and the hydrolysis of the methyl ester of compound **2** were performed in a single step in HCl 3 M at reflux overnight. This led to **L5** as a chlorohydrate salt with a yield of 95%. The complete characterizations by NMR and HR-MS are given in Figures S3-S5 (Supporting Information). Complexation reactions were carried out using 1.3 equiv. of Y(III) or Ln(III) salts (Ln = Eu, Tb, Gd) at pH 6 and 100°C for 14h (HRMS characterizations in Figures S7-S10, Supporting Information).

The synthesis of the second regioisomer, ligand **L6**, was performed in three steps from pyclen alloc **3** that was recently described by some of us (Scheme 2).[23] Alkylation with two equivalents of the picolinate arm on the latter afforded compound **4** in 71% yield. Removal of the Alloc group with phenylsilane catalyzed by $Pd(PPh_3)_4$ followed by a quick purification by column chromatography on activated alumina proved to be very

efficient, since pyclen derivative **5** was obtained in 90% yield. All intermediate compounds were characterized by ^{1}H and ^{13}C NMR (Figure S11-S16). Finally, hydrolysis of the methyl esters under acidic conditions (HCl, 6M) at reflux led to the ligand **L6**·xHCl in 60% yield after several precipitations. The chlorohydrate salt was characterized in solution by ^{1}H and ^{13}C NMR (Figures S17-18). Its purity was also verified by analytical HPLC (Figure S19) and by high-resolution mass spectrometry (electrospray ionization, Figure S20). As for **L5**, **L6** was engaged in complexation reactions with metal chloride salts (pH 6, 100°C, 14 h) to afford the corresponding [M**L6**]$^{+}$ chelates with high yields (Scheme 2). Their formation and purity was checked by HR-ESI and subsequently used for further studies (Figures S21-S24).

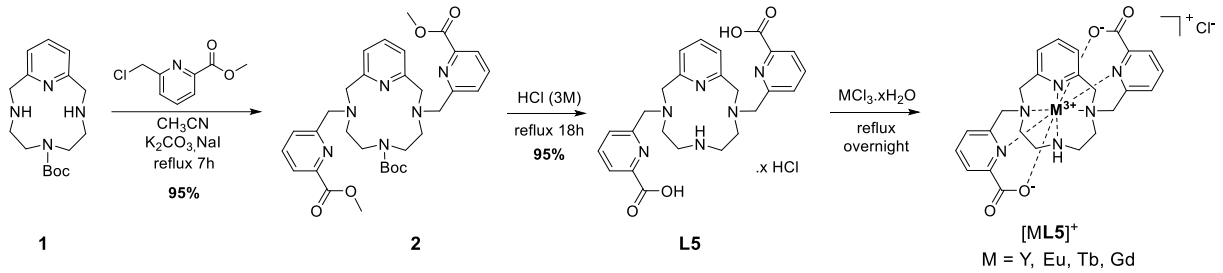

Scheme 1. Synthesis of [M**L5**]$^{+}$ metal complexes from pyclen-boc **1**.

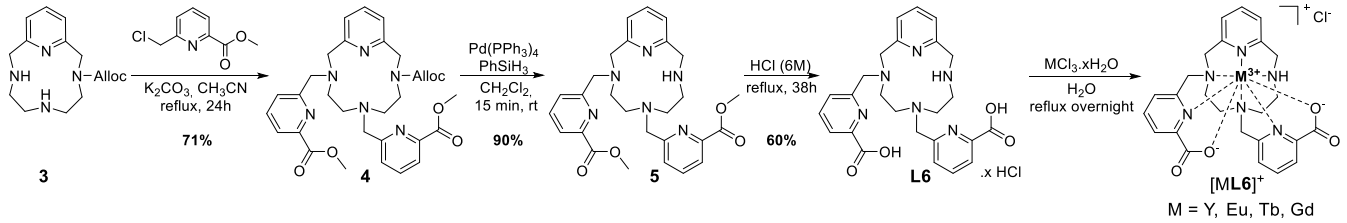

Scheme 2. Synthesis of [M**L6**]$^{+}$ metal complexes from pyclen-alloc **3**.

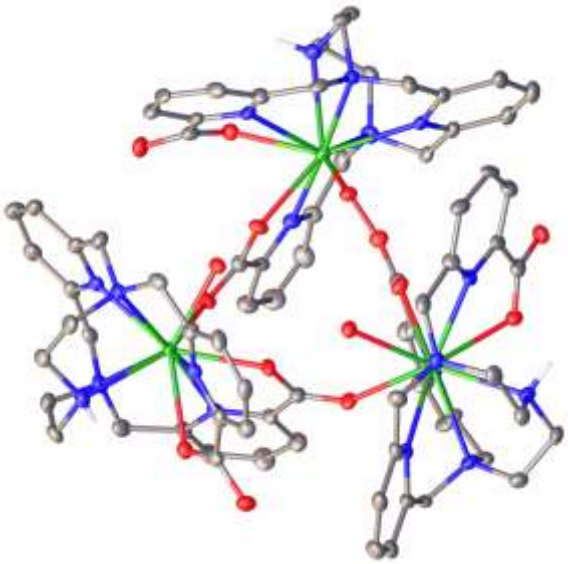

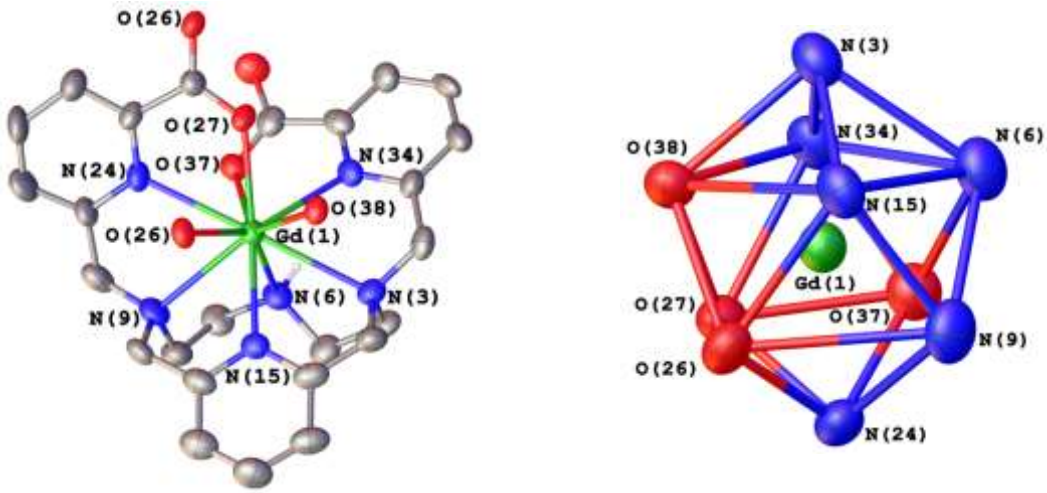

Figure 1. Crystal structure of the trinuclear species $[(Gd\mathbf{L5})_3(H_2O)_3]^{3+}$ (top) and detail of one of the monomeric unit and the corresponding coordination polyhedron, including the numbering scheme (bottom). Hydrogen atoms bonded to C atoms and anions have been omitted for simplicity. The ORTEP plots are at the 50% probability level.

X-ray crystal structure. The slow evaporation of an aqueous solution of the $[Gd\mathbf{L5}]^+$ complex provided single crystals appropriate for X-ray diffraction measurements. Crystals were found to contain the trinuclear entity $[(Gd\mathbf{L5})_3(H_2O)_3]^{3+}$, perchlorate and chloride anions, ammonium cations and water molecules. The compound crystallizes in the cubic $F\bar{4}3c$ space group. The three $[Gd\mathbf{L5}(H_2O)]^+$ units present in the trinuclear edifice are related by a C_3 symmetry axis and thus present identical bond distances (Table 1) and angles. The $[Gd\mathbf{L5}(H_2O)]^+$ units are joined by bridging carboxylate units that coordinate through an asymmetrical μ_2-η^1:η^1 mode [Gd(1)-O(26) = 2.492(10) Å; Gd(1)-O(27) = 2.423(8) Å],[24] where the oxygen atom that joins the three mononuclear entities [O(26)] provides the longest distance to the metal ion. A similar trinuclear structure was observed both in the solid state and in solution for lanthanide complexes formed with dipicolinate cyclen derivatives.[16] Dinuclear structures supported by asymmetrical μ_2-η^1:η^1 picolinate coordination were also reported.[18a,25] In the trinuclear $[(Gd\mathbf{L5})_3(H_2O)_3]^{3+}$ entity, each Gd(III) center is coordinated to the four nitrogen atoms of the pyclen scaffold, two nitrogen atoms of the picolinate groups, two oxygen atoms of picolinate carboxylate groups and an oxygen atom of a carboxylate function from a neighbor $[Gd\mathbf{L5}]^+$ moiety. Ten-coordination is completed by the presence of an inner-sphere water molecule [Gd(1)-O(38) = 2.428(9) Å] involved in hydrogen bonding with a chloride anion [O(38)···Cl(4), 3.131(10) Å; H(38w)···Cl(4), 2.30(4); O(38)-H(38w)···Cl(4), 158(8)º].

The coordination polyhedron around the metal ion can be best described as a bicapped square antiprism, as confirmed by shape measures performed with the SHAPE program.[26,27] One of the quadrangular faces of the square antiprism is defined by O(38), N(15), N(6) and N(34) (rms 0.079 Å), while the second quadrangular face is delineated by N(9), O(26), O(27) and O(37) (rms 0.024 Å). The mean square planes are nearly parallel, intersecting at 3.2º. The two quadrangular faces are twisted with respect to each other with an average twist angle of 44.6º, a value that is very close to the ideal one for a square antiprism (45º). The donor atoms that occupy the capping positions define a nearly linear angle with the metal ion [N(3)-Gd(1)-N(24) = 175.9(3)º]. A bicapped square antiprismatic coordination was observed previously for the Gd(III) complex with a non-macrocyclic octadentate picolinate ligand,[28] as well as for $[Eu\mathbf{L3}]$.[18]

Table 1. Bond distances (Å) of the metal coordination environments obtained for the $[(GdL5)_3(H_2O)_3]^{3+}$ entity with X-ray diffraction measurements.

bond	Bond distance	bond	Bond distance
Gd(1)-N(3)	2.767(11)	Gd(1)-N(34)	2.568(10)
Gd(1)-N(6)	2.597(12)	Gd(1)-O(38)	2.428(9)
Gd(1)-N(9)	2.718(11)	Gd(1)-O(26)	2.492(10)
Gd(1)-N(15)	2.500(10)	Gd(1)-O(27)	2.423(8)
Gd(1)-N(24)	2.616(10)	Gd(1)-O(37)	2.523(10)

The coordination of the macrocyclic pyclen unit results in the formation of four five-membered chelate rings that yield an unusual (δλδδ) [or (λδλλ)] conformation,[29] instead of the more common (δλδλ) observed in complexes of the lanthanide and other large metal ions with pyclen-based ligands.[18a,30] The structures of 10-coordinate Gd(III) complexes containing picolinate groups reported so far present a rather broad range of Gd-O (2.32-2.52 Å) and Gd-N (2.52-2.65 Å) distances involving the carboxylate and pyridyl donor atoms.[13a,18a,28] This likely reflects some degree of steric hindrance to reach ten-coordination, which is relatively abundant for the largest lanthanides but rare for the second half of the series.[31]

NMR investigations in aqueous solution. NMR studies of the diamagnetic analogues $[Y\mathbf{L5}]^+$ and $[Y\mathbf{L6}]^+$ were performed in D_2O solution to gain insight into the structures of this family of complexes. The ^1H and ^{13}C NMR spectra and the signal attribution are given in Figures S25-S30 and Tables S1-S2 (Supporting Information). The ^1H NMR spectra are well resolved, and point to a rather rigid structure of the complexes in solution. The ^{13}C NMR spectra present 25 signals for both $[Y\mathbf{L5}]^+$ and $[Y\mathbf{L6}]^+$, as would be expected for a C_1 symmetry in solution.

This indicates that these complexes exist as a single diastereoisomer in solution with no fluxionality at room temperature on the NMR timescale, a desirable property that usually correlates with high stability.[32]

Diffusion-ordered NMR spectroscopy (DOSY) experiments in D_2O were carried out to investigate the potential formation of aggregates in aqueous solution (Figures S31-S35, Supporting Information). These studies provided very similar diffusion coefficients for both Y(III) chelates (D = 2.9x10^{-10} m^2.s^{-1} for [Y**L5**]$^+$ and D = 3.0x10^{-10} m^2.s^{-1} for [Y**L6**]$^+$, at 298 K). A van der Waals radius of a = 5.9 Å can be deduced for both Y(III) chelates from these diffusion coefficients using Eq (1),[33] where k_B represents the Boltzmann constant, T is the absolute temperature and η is the viscosity of the medium (η_{D2O} = 1.232 × 10^{-3} Pa s at 298 K).[34]

$$D = \frac{k_B T}{6\pi a \eta} \qquad (1)$$

The diffusion coefficients obtained for these complexes are close to those reported for mononuclear lanthanide complexes with similar size.[35] Furthermore, the volume of the trinuclear edifice observed in the solid state for the Gd(III) complex was estimated to be 1610 Å^3 with the aid of DFT calculations, which corresponds to a sphere with a radius of 7.3Å. This radius is considerably longer than that estimated from the diffusion coefficient (5.9 Å), indicating the presence of monomeric entities in aqueous solutions.

Further information on the metal coordination environment in the Y(III) complexes can be obtained by measuring ^{89}Y NMR shifts, which were collected using ^{1}H,^{89}Y-HMQC spectroscopy.[36] This allows a fast acquisition of shift data in comparison with conventional ^{89}Y NMR, which requires using long delay times due to the very slow nuclear relaxation of ^{89}Y.[37] ^{89}Y NMR chemical shifts of δ = 154 ppm and 135 ppm were measured for [Y**L5**]$^+$ and [Y**L6**]$^+$, respectively (Figure S31-S32). Thus, the ^{89}Y NMR signal of [Y**L5**]$^+$ is deshielded by ~20 ppm in comparison to [Y**L6**]$^+$.

As previously demonstrated by some of us, ^{89}Y NMR chemical shifts are highly dependent of the coordination environment (i.e number and nature of the donor atoms of the ligand), and therefore give useful information on the structure of Y(III) complexes and their Ln(III) analogues in solution.[38] Indeed, an empirical expression [Eq (2)] was developed relating the nature of the donor atoms coordinated to Y(III) and the ^{89}Y NMR chemical shift:

$$\delta^{calc}(^{89}Y) = 863 - (S_{Nam}\cdot n_{Nam} + S_{Npy}\cdot n_{Npy} + S_{Oc}\cdot n_{Oc} + S_{Ow}\cdot n_{Ow}) \qquad (2)$$

Where S_{Nam}, S_{Npy}, S_{Oc} and S_{Ow} are the shielding contributions of amine, pyridine, carboxylate and water donor atoms (68.1, 85.7, 94.0 and 107.6 ppm, respectively), and n_{Nam}, n_{Npy}, n_{Oc} and n_{Ow} are the number of donor atoms of each type. In previous works, we showed that the shielding constant of the pyridine N atom of pyclen was similar to that of amine N atoms (68.1 ppm).[39] Furthermore, the relaxometric and luminescent properties of the Gd(III) and Tb(III) complexes point to the presence of a water molecule coordinated to the metal ion (see below). Thus, the ^{89}Y NMR shifts of [Y**L5**]$^+$ and [Y**L6**]$^+$ can be estimated with Eq (2) using n_{Nam} = 4, n_{Npy} = 2, n_{Oc} = 2 and n_{Ow} = 1, yielding δ = 124 ppm. This value is in excellent agreement with the experimental shift measured for [Y**L6**]$^+$, with a deviation of 11 ppm. This agreement is remarkable considering that the chemical shifts of complexes with polyaminocarboxylate ligands expand up to 270 ppm.[38] For [Y**L5**]$^+$, the deviation is somewhat larger, reflecting that the nature of the donor atoms is not the only factor affecting the ^{89}Y chemical shifts.

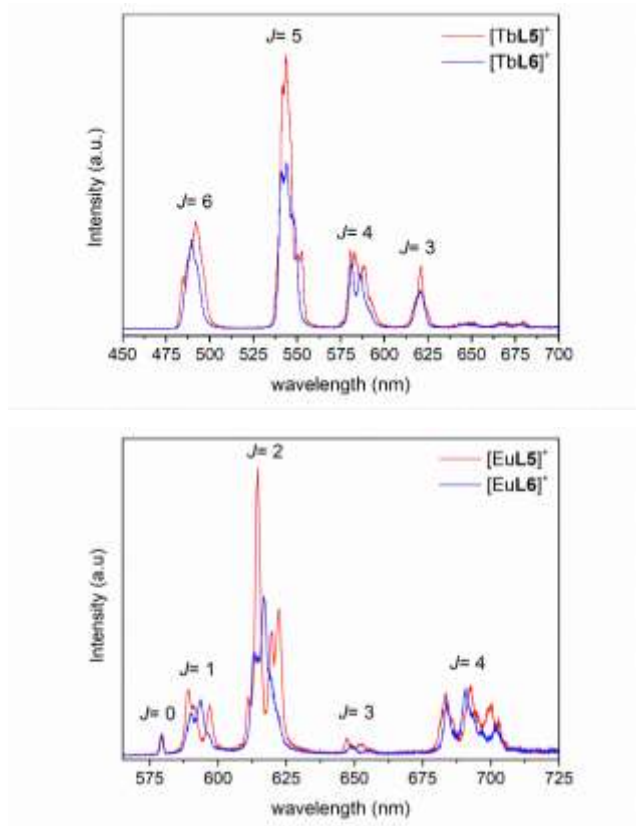

Figure 2. Metal-centered emission of the Tb(III) (top) and Eu(III) complexes (bottom) formed with ligands **L5** and **L6** (1×10^{-5} M) recorded under excitation at 272 nm (Tris/HCl 0.1 M, pH 6.8, 25 ºC).

Photophysical Properties. The absorption spectra of the [Tb**L5**]$^+$ and [Tb**L6**]$^+$ complexes present an absorption maximum at 269 nm (ε ~ 9800 M^{-1} cm^{-1}) typical of the picolinate chromophore (Figure S35, Supporting Information).[40,41] The emission spectra recorded upon excitation in the ligand bands (272 nm) show the typical $^5D_4 \rightarrow {}^7F_J$ transitions of Tb(III), which are observed at ca. 490 (J = 6), 544 (J = 5), 583 (J = 4) and 621 (J = 3) nm (Figure 2). The emission spectra of the two complexes are similar, being dominated by the $^5D_4 \rightarrow {}^7F_5$ transition. The lifetimes of the excited $^5D_4$ state were determined using the time-correlated single photon counting method, which afforded mono-exponential decays both in H_2O and D_2O solutions (Table 2, Figures S36-S39, Supporting Information). The hydration number (q), estimated from these lifetime measurements with the aid of the empirical correlation proposed by Beeby,[42] points to the presence of one water molecule coordinated to the metal ion (Table 2). Thus, these complexes are very likely nine-coordinated in aqueous solutions, with a coordination environment

fulfilled by eight donor atoms of the ligand (the four donor atoms of the pyclen unit and the four provided by the picolinate pendants), together with the oxygen atom of a coordinated water molecule. The lifetimes measured in H_2O are slightly shorter than those measured for the [Tb**L1**] and [Tb**L2**] analogues,[18] which also contain a coordinated water molecule. This might reflect some quenching effect in the [Tb**L5**]$^+$ and [Tb**L6**]$^+$ complexes originated from the amine N-H oscillators. Longer lifetimes of up to 2.5 ms were reported for non-hydrated picolinate complexes.[18a,40]

Table 2. Spectroscopic Properties of the Eu(III) and Tb(III) Complexes of Ligands L5 and L6.[a]

	τ_{H_2O} / ms [b]	τ_{D_2O} / ms [b]	Φ / % [c]	q [d]
[Eu**L5**]$^+$	τ_1= 0.385 (97%)	τ_1= 0.587 (89%)	8	0.8
	τ_2= 1.03 (3%)	τ_2= 1.77 (11%)		0.2
[Eu**L6**]$^+$	τ_1= 0.430 (95%)	τ_1= 0.758 (82%)	8	0.9
	τ_2= 0.868 (5%)	τ_2= 2.01 (18%)		0.5
[Tb**L5**]$^+$	1.36	1.96	50	0.8
[Tb**L6**]$^+$	1.45	2.28	34	1.0

[a] Data in Tris/HCl 0.1 M, pH 6.8, 25 ºC. [b] Fits to biexponential decays are provided when monoexponential decays provide poor fits. [c] Calculated using the Eu^{3+} and Tb^{3+} tris(dipicolinate) complexes as secondary standard, ref. 43. [d] Calculated according to ref.42.

The emission quantum yields (Φ) of [Tb**L5**]$^+$ and [Tb**L6**]$^+$ were determined using the corresponding tris(dipicolinate) complex as standard.[43] Both complexes present high emission quantum yields (53 and 22%, respectively), with values similar to those determined for [Tb**L1**] and [Tb**L2**], but lower than those reported for the q = 0 analogues [Tb**L3**] and [Tb**L4**] (90%).[18a] Quantum yields of ca. 20-40% were reported for other monohydrated Tb(III) complexes with picolinate ligands,[44] which demonstrates the high efficiency of the picolinate chromophore to sensitize the Tb(III) emission.

The emission spectra of the [Eu**L5**]$^+$ and [Eu**L6**]$^+$ complexes present the characteristic $^5D_0 \rightarrow {}^7F_J$ (J = 0-4) transitions of Eu(III) complexes,[45] in which the emission intensity is dominated by the $\Delta J = 2$ transition . The spectra of the two complexes present rather different splitting patterns of the $\Delta J = 1$ transitions (Figure 2), as well as different intensity ratios of the $\Delta J = 2$ and $\Delta J = 1$ transitions (ΔJ=2/ΔJ= 1 = 3.2 and 2.8 for [Eu**L5**]$^+$ and [Eu**L6**]$^+$, respectively). The intensity of the electric dipole $\Delta J = 2$ transition was found to be very sensitive to the coordination environment around the Eu(III) ion, while the intensity of the $\Delta J = 1$ transition is rather insensitive to changes in the metal coordination sphere.[46,47] Thus, these results indicate that the [Eu**L5**]$^+$ and [Eu**L6**]$^+$ complexes present rather different coordination environments.

The emission decays obtained for the Eu(III) complexes in H_2O and D_2O solutions could not be fitted to monoexponential decays. The fit of the data to biexponential decay expressions afforded the lifetimes reported in Table 2 (Figures S40-S41, Supporting Information). This suggests that two emissive species with significantly different lifetimes are present in solution. The major emissive species (> 80%, Table 2) present a shorter emission lifetime. The application of the empirical expression developed by Beeby[42] yields hydration numbers close to 1, in line with the results obtained for the Tb(III) analogues. The lifetimes obtained for the minor species provide lower hydration numbers, though these q values must be taken with some care. The emission quantum yields determined for both complexes (8%) are similar to those reported for other monohydrated Eu(III) complexes with picolinate ligands.[44b]

^{1}H relaxivity and water exchange kinetics. The efficiency of a paramagnetic chelate to enhance the relaxation rates of water protons is generally assessed in vitro using relaxivity (r_{1p}) measurements. The r_{1p} values of [Gd**L5**]$^+$ and [Gd**L6**]$^+$ were obtained from the slopes of the plots of the longitudinal relaxation rates ($1/T_1$) versus complex concentration measured at 20 and 60 MHz and 298 K (Figures S41-S42, Supporting Information). The r_{1p} values for the two magnetic field strengths were found to be 4.46 (20 MHz) and 4.47 $mM^{-1}s^{-1}$ (60 MHz) for [Gd**L5**]$^+$, and 4.35 (20 MHz) and 4.12 $mM^{-1}s^{-1}$ for [Gd**L6**]$^+$. These values are in the same order of magnitude as mono-hydrated Gd(III) chelates of similar size such as the well-known [Gd(dota)]$^-$ (r_{1p} = 4.2 $mM^{-1}s^{-1}$ at 20 MHz and 298 K).[53] This supports the formation of mononuclear and monohydrated [Gd**L5**]$^+$ and [Gd**L6**]$^+$ complexes in solution, in agreement with the luminescence lifetimes determined for the Tb(III) and Eu(III) analogues.

An important parameter that affects the relaxivity of Gd(III) chelates is the exchange rate of the coordinated water molecule(s). The water exchange rates determined for Gd(III) complexes were found to cover a broad range of four orders of magnitude,[48] with the faster exchange rate corresponding to the aquated ion $[Gd(H_2O)_8]^{3+}$ (k_{ex}^{298} = 830×10^6 s^{-1}).[49] The lowest k_{ex}^{298} values were reported for dota-tetraamide derivatives (~0.1×10^6 s^{-1}).[50] The water exchange rates of the coordinated water molecule present in [Gd**L5**]$^+$ and [Gd**L6**]$^+$ complexes were investigated using ^{17}O NMR transverse relaxation rates recorded at variable temperatures (Figure 3). The reduced transverse relaxation rates ($1/T_{2r}$) measured for [Gd**L5**]$^+$ and [Gd**L6**]$^+$ display an opposite temperature dependence. Merbach and coll. showed that the temperature dependence of reduced transverse relaxation rates can be rationalized using the simplified Eq (3):[51]

$$\frac{1}{T_{2r}} = \frac{1}{T_{2m}+\tau_m} \qquad (3)$$

Where T_{2m} is the transverse relaxation time of the bound water molecule and τ_m is the mean residence time of a water molecule in the inner coordination sphere of Gd(III) ($\tau_m = 1/k_{ex}$). Usually, T_{2m} increases when the temperature increases while τ_m shows the opposite behavior. For [Gd**L5**]$^+$, $1/T_{2r}$ decreases with temperature, a situation that is characteristic of the fast exchange regime, in which $T_{2m} >> \tau_m$. The opposite holds for [Gd**L6**]$^+$, where τ_m dominates the denominator of Eq (3). This qualitative analysis indicates that these two complexes are characterized by very different water exchange rates.

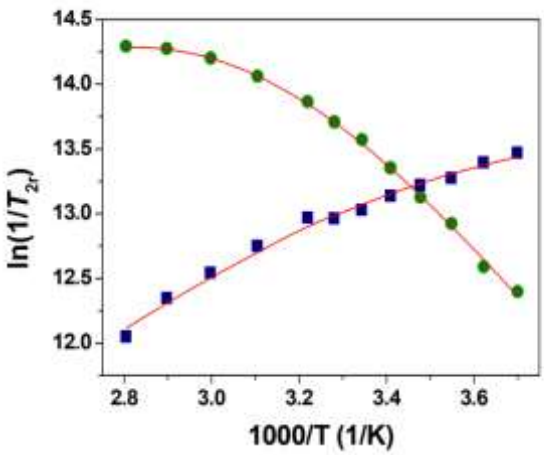

Figure 3. Reduced transverse ^{17}O relaxation rates measured at 9.4 T (pH = 7.4) for [Gd**L5**]$^+$ (squares) and [Gd**L6**]$^+$ (circles). The solid line corresponds to the least-squares fit of the data as described in the text.

The $1/T_{2r}$ data were fitted using standard methods, including the water exchange rate at 298 K (k_{ex}^{298}), its activation enthalpy ($\Delta H^{\neq}$) and the relaxation rate of the electron spin ($1/T_{1e}^{298}$) as fitting parameters. The activation energy of electron spin relaxation was fixed to 1 kJ/mol, as otherwise the fits afforded small negative values. Finally, the value of the scalar hyperfine coupling constant $A_O/\hbar$ was set to the standard value of -3.8x10^6 rad·s^{-1}.[52]

The contribution of the electronic relaxation to the correlation time ($1/\tau_c = k_{ex} + 1/T_{1e}$) was estimated for both systems in the temperature range investigated. Based on the results the contribution of the water exchange rate at 348 K is more than 81% for [Gd**L5**]$^+$, while only a bit more than 20% for [Gd**L6**]$^+$. This makes the determination of k_{ex} for [Gd**L6**]$^+$ less accurate. Nevertheless, the fit of the data yields very different k_{ex}^{298} values for [Gd**L5**]$^+$ and [Gd**L6**]$^+$. Water exchange is very fast in [Gd**L5**]$^+$, with k_{ex}^{298} being ~20 times higher than for [Gd(dota)]$^-$ (Table 3).[53] The bis-hydrated [Gd(pcta)] complex also presents a lower water exchange rate compared to [Gd**L5**]$^+$.[54] On the contrary, water exchange in [Gd**L6**]$^+$ is lower than in [Gd(dota)]$^-$. Different water exchange rates were also determined for the regioisomeric complexes [Gd**L1**] and [Gd**L2**], but the effect was not as pronounced as for [Gd**L5**]$^+$ and [Gd**L6**]$^+$.[19] Fast water exchange was observed previously for [Gd(do2pa)]$^+$ and [Gd(bp12c4)]$^+$, which are structurally related to [Gd**L5**]$^+$.[15,16] In the case of [Gd(do2pa)]$^+$, steric compression around the water binding site was identified as a key factor that favors fast water exchange, which follows a dissociative mechanism.

The analysis of ^{17}O NMR data also gave access to T_{1e}^{298}, the relaxation times of the electron spin, at 298K. The T_{1e}^{298} value obtained for [Gd**L5**]$^+$ (7.2×10^7 s^{-1}) is twice as high than for [Gd**L6**]$^+$ (3.27×10^7 s^{-1}), which shows that the different metal coordination environments present in the two complexes have a significant impact in the relaxation of the electron spin.[55] These complexes appear to present faster relaxations of the electron spin than [Gd(dota)]$^-$ (Table 3), probably due to the lower symmetry of the metal coordination environment.[56]

Additional insight into the reasons for the different water exchange rates in the [Gd**L5**]$^+$ and [Gd**L6**]$^+$ complexes was obtained with the aid of DFT calculations. These calculations provide the optimized geometries shown in Figure 4, which include two explicit second-sphere water molecules to obtain more accurate Gd-O$_{water}$ distances and $A_O/\hbar$ values.[52] The optimized geometries of the two complexes contain a pyclen fragment that adopts a (δλδλ) conformation, with coordination polyhedra those can be described as tricapped trigonal prisms. The oxygen atom of the coordinated water molecule in [Gd**L6**]$^+$ defines one of the vertexes of the trigonal prism, while in [Gd**L5**]$^+$ the coordinated water molecule is capping one of the rectangular faces of the prism. As a result, the coordinated water molecule in [Gd**L5**]$^+$ is in a sterically demanding position, which results in a long Gd-O$_{water}$ bond (2.483 Å) in comparison to [Gd**L6**]$^+$ (2.452 Å). Thus, the high water exchange in [Gd**L5**]$^+$ is related to a high steric compression around the water binding site, which favors the dissociative water exchange mechanism. This is in line with our recent studies, which demonstrated that water molecules occupying capping positions in the coordination polyhedron are particularly labile.[57] Our DFT calculations yield $A_O/\hbar$ values for the coordinated water molecule of 3.88×10^6 rad s^{-1} and 4.23×10^6 rad s^{-1} for [Gd**L5**]$^+$ and [Gd**L6**]$^+$, respectively. These values are close to those determined for different Gd(III) complexes ($A_O/\hbar$ = -3.8 ± 0.2 ×10^6 rad s^{-1}),[53,58] and support the analysis of the ^{17}O NMR data described above.

Thermodynamic stability constants. The protonation constants of the ligands **L5** and **L6** were determined by potentiometric measurements (I = 0.15 M NaCl, 25°C), whereas the stability constants of the corresponding Gd(III) complexes were accessed by using relaxometic titrations on equilibrated samples (batch method). The data obtained are compared in Table 4 with those of the family of picolinate acetate pyclen derivatives (**L1**-**L4**) and some other chelators commonly used for Gd(III) complexation.

The protonation constants and overall basicities of the ligands, estimated as $\sum_{i=1}^{4} logK_i^H$, are given in Table 4. The protonation sequence of pyclen derivatives was investigated in detail for pcta.[59] According to these studies, the first protonation occurs on the amine N atom opposite to the pyridine ring. This explains the lower protonation of **L6**, compared to **L5** (log $K1$ = 9.91 and 12.07 for **L6** and **L5**, respectively), which is associated to the electron withdrawing effect of the picolinate group.[28,60] The pyclen-based ligands containing a carboxylate function on the amine N opposite to the pyridine ring (**L2** and **L3**) present higher log $K1$ values than those incorporating picolinate groups, which shows that the picolinate group is more electron withdrawing than the acetate function.[61] The overall basicities of **L5** and **L6** are in the range observed for N-functionalized pyclen derivatives, being considerably lower than for dota.[62]

Table 3. ^{1}H relaxivities (r_{1p}, 20 MHz, 298 K) and best-fit parameters obtained from the analysis of ^{17}O NMR transverse relaxation rates and for [GdL5]$^{+}$, [GdL6]$^{+}$ and related systems.

	$\Delta H^{\ddagger}$ / kJ mol^{-1}	k_{ex}^{298} / $\times 10^{6}$ s^{-1}	$1/T_{1e}^{298}$ / $\times 10^{7}$ s^{-1}	r_{1p} / mM^{-1}s^{-1}	Reference
L5 [a]	18.4±2.4	87.1±14	7.2±1.3	4.46	This work
L6 [a]	31.7±0.7	1.06±0.02	3.27+0.09	4.35	This work
L1 [b]	28.6	1.08	2.02	4.74	19
L2 [b]	37.5	22.5	2.79	4.95	19
dota	49.8	4.1	0.25[b]	4.2	53
pcta	45	14.3	0.69[b]	7.09	54
do2pa	30.7	58	1.17[b]	3.23	16
bp12c4	14.8	220	1.9[c]	-	15

[a] Values obtained at 9.4 T. [b] Calculated from the values of the mean-square zero field splitting energy (Δ^2) and the correlation time for the modulation of the zero field splitting (τ_v). [c] Value at 11.75 T.

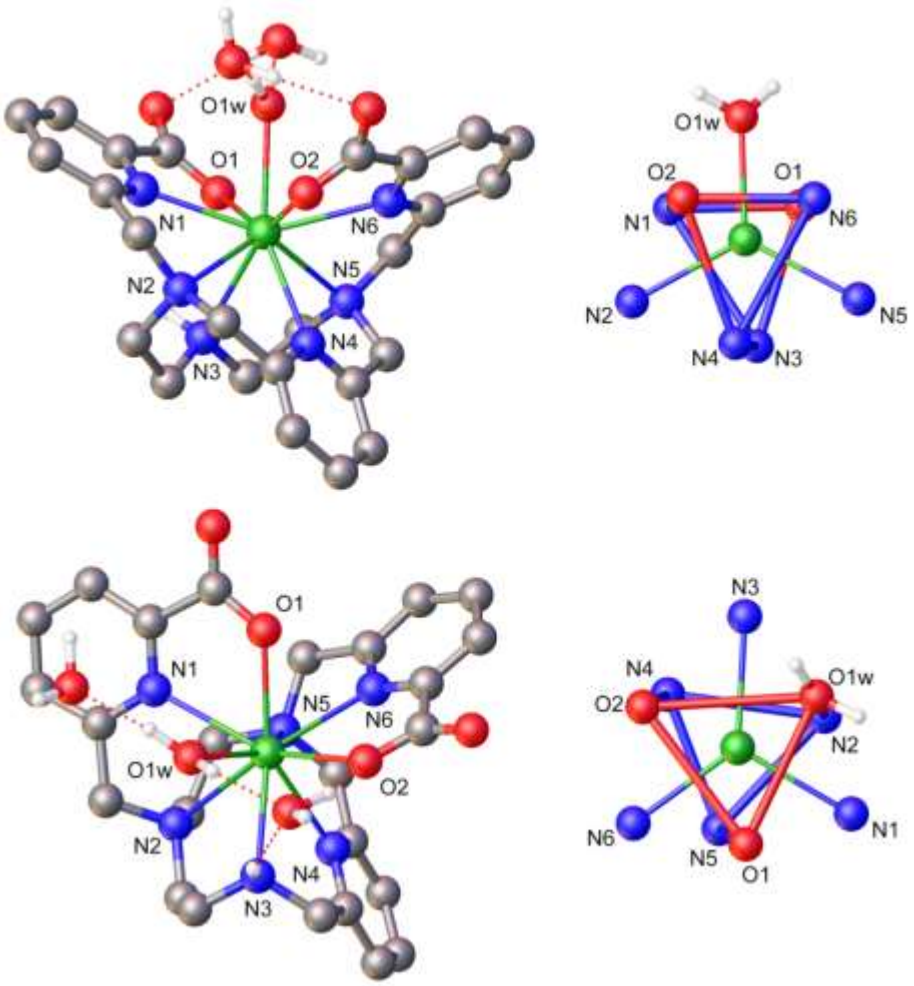

Figure 4. Structures of the [Gd**L5**(H2O)]$^{+}$·2H$_2$O (top) and [Gd**L6**(H$_2$O)]$^{+}$·2H$_2$O (bottom) systems obtained with DFT calculations and views of the corresponding coordination polyhedra.

Table 4. Protonation constants of L5 and L6 and stability constants of their Gd(III) chelates compared with ligands of reference (25°C).

	L5[a]	**L6**[a]	**L1**[b]	**L2**[b]	**L3**[c]	**L4**[c]	**dota**[d]	**pcta**[b]	**do2pa**[e]	**bp12c4**[f]
log K_1	12.07(1)	9.91(1)	9.69	10.43	11.22	9.90	12.09	9.97	11.16	9.16

log K_2	5.18(4)	8.37(1)	7.63	6.47	5.96	6.81	9.68	6.73	10.11	7.54
log K_3	4.35(4)	3.90(1)	4.02	4.13	4.42	3.96	4.55	3.22	4.06	3.76
log K_4	2.02(4)	2.77(1)	2.35	2.71	3.17	3.12	4.13	1.4	3.50	2.79
log K_5	-	-	-	-	1.89	1.70	-	-	0.90	
$\sum_{i=1}^{4} \log K_i^H$	23.62	24.95	23.69	23.74	24.77	23.79	30.45	21.32	28.83	23.25
logK_{GdL}	20.47(5)	19.77(8)	20.49	22.37	23.56	23.44	24.7	18.28	17.27	18.82
pGd[g]	16.76	17.20	18.74	20.25	20.69	21.83	19.21	16.62	11.75	17.63

[a] This work (I = 0.15 M NaCl). [b] Ref 19 (I = 0.15 M NaCl). [c] Ref 18a (I = 0.15 M NaCl). [d] Ref 62 (I = 0.15 M Me_4NNO_3). [e] Ref 16 (I = 0.15 M NaCl). [f] Ref 15 (I = 0.1 M KCl). [g] pGd values were calculated by using the conditions proposed by Raymond *et al.* (pH = 7.4, c_{Lig} = 10×$c_{Gd(III)}$ = 10^{-5} M), ref 63.

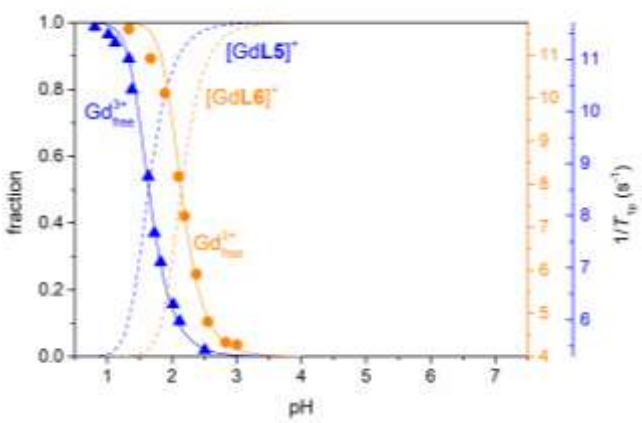

Figure 5. Proton relaxation times (T_{1p}) of [Gd**L5**]$^+$ (triangles) and [Gd**L6**]$^+$ (circles) as a function of pH, and species distributions calculated with the stability constants given in Table 4 (25 ºC, 0.15 M NaCl).

The proton relaxation times recorded from solutions of the [Gd**L5**]$^+$ and [Gd**L6**]$^+$ complexes over the 0.7 to 4 pH range are presented Figure 5. Below pH~2, the relaxivity of aqueous solutions of the complexes increases since the complexes progressively dissociate into $[Gd(H_2O)_8]^{3+}$ as the pH decreases. Surprisingly, a lower pH is required to fully dissociate [Gd**L5**]$^+$ than to dissociate [Gd**L6**]$^+$ and to reach the specific relaxivity of 11.5 $mM^{-1}\cdot s^{-1}$ corresponding to $[Gd(H_2O)_8]^{3+}$ aqua complex at 60 MHz and 298 K.**Erreur ! Signet non défini.**

The stability constants of the [Gd**L6**]$^+$ complex (log K_{GdL} = 19.77) is slightly lower than that of [Gd**L5**]$^+$ (log K_{GdL} = 20.47). The latter value is very similar to that reported for [Gd**L1**] and 2-3 log K units lower than those reported for the complexes of **L2**, **L3** and **L4** (Table 4).[18a,19] The stabilities of [Gd**L5**]$^+$ and [Gd**L6**]$^+$ are however higher than that of [Gd(pcta)] determined using the same conditions.[19] A lower stability constant was also reported for [Gd(do2pa)]$^+$ (log K = 17.27, 0.15 M NaCl),[16] the cyclen-based analogue of [Gd**L5**]$^+$. The [Gd**L5**]$^+$ complex is also more stable than [Gd(bp12c4)]$^+$,[15] which contains a 1,7-diaza-12-crown-4 macrocyclic unit. These results show that the pyclen platform yields more stable complexes than those based on 12-membered macrocycles such as cyclen and diaza-12-crown-4 functionalized with the same pendant arms. Nevertheless, the comparison of the log K_{ML} values does not reflect the effect of ligands basicity on complex formation. Thus, we used the thermodynamic stability constants listed in Table 4 to calculate pGd values, defined as -log$[Gd]_{free}$ at pH = 7.4 with c_L=10×c_{Gd}=10^{-5} M,[63] which take into account the competition between protonation and metal binding. The calculation of the pGd values for [Gd**L5**]$^+$ and [Gd**L6**]$^+$ shows that these complexes present stabilities at pH 7.4 comparable to those of [Gd(pcta)] and [Gd(bp12c4)]$^+$, but higher than that of [Gd(do2pa)]$^+$, which is clearly related to the higher basicity of the ligand in the latter. The species distribution diagrams shown in Figure 5 show that there is no free Gd(III) above pH 3.2, in line with a high stability of the complexes.

Table 5. Rate and equilibrium constants characterizing the dissociation rates of [GdL5]$^+$ and [GdL6]$^+$ complexes and comparison with reference Gd(III) chelates (I = 1.0 M (Na$^+$ + H$^+$)Cl-, T = 25 °C).

	k_1 / M^{-1} s^{-1}	K_1^H / M^{-1} [b]	$t_{1/2}$ / min [c]
L5 [a]	(6.82±0.09)×10^{-5}	0.34±0.02	5151
L6 [a]	(1.05±0.02)×10^{-3}	0.57±0.03	204
L1 [b]	6.9×10^{-4}	-	167
L2 [b]	2.13×10^{-4}	-	542
L3 [c]	1.45×10^{-4}	0.60	1408
L4 [c]	6.3×10^{-7}	-	76000
dota [d]	1.83×10^{-6}	-	64000
pcta [b]	5.08×10^{-4}	-	231
do2pa [e]	2.5×10^{-3}	-	10.7
bp12c4 [f]	0.126	39.8	0.11

[a] This work. [b] Ref. 19. [c] Ref. 18a. [d] Ref. 64. [e] Ref. 16. [f] Ref. 15.

Dissociation kinetics of Gd(III) Complexes. The rates of dissociation of metal complexes, specially of Gd(III) ones, is an important parameter to consider for their safe use in medical applications.[64] Even if acidic conditions are not representative of biological media, the study of dissociation kinetics in strong acids allows for the good comparison between chelates (this can

also be rationalized in terms of very low reaction rates when approaching the physiological conditions). Thus, the acid catalyzed dissociation rates of [Gd**L5**]$^+$ and [Gd**L6**]$^+$ were investigated at the 0.1 to 1.0 M proton concentration at 25 °C (Figure 6). The rather high proton concentration ensures pseudo-first-order conditions, so that the rates of dissociation can be expressed as in Eq (4):

$$\frac{-d[\mathrm{GdL}]_\mathrm{t}}{dt} = k_\mathrm{d}[\mathrm{GdL}]_\mathrm{t} \qquad (4)$$

Under highly acidic conditions, the complexes are thermodynamically not stable and fall apart by forming multi-protonated ligands and releasing the metal ion. For the dissociation to happen, the complex needs to be protonated at a site which is weakly bound to the metal center, while with time this proton is expected to "migrate" to the most basic donor atom in the ligand (these are the nitrogen atoms of the macrocycle) achievable *via* structural rearrangements. Meanwhile, the metal ion leaves the cavity of the macrocycle. The plots of k_{obs} as a function of proton concentration indicate that the [Gd**L5**]$^+$ complex undergoes slower dissociation in acidic conditions than [Gd**L6**]$^+$ (Figure 6). The saturation-like behavior observed for k_{obs} on increasing proton concentration suggests that the dissociation of the Gd(III) complexes proceeds *via* the formation of mono- and di-protonated intermediate complexes. Taking into account the concentration of these complexes, the rate of dissociation can be given as in Eq (5), where k_0 is the rate constant characterizing the spontaneous dissociation of the complex, while k_1 is the rate constant characterizing the acid assisted dissociation of the monoprotonated complex formed in the presence of high concentrations of acid.

$$-\frac{d[\mathrm{GdL}]}{dt} = k_d[\mathrm{GdL}]_t = k_0[\mathrm{GdL}] + k_1[\mathrm{GdHL}] \qquad (5)$$

Considering that the total concentration of complex $[\mathrm{GdL}]_t$ = [GdL] + [GdHL], and the expression of the protonation constant ($K1^\mathrm{H}$= [GdHL]/([GdL][H$^+$]), one can obtain the following expression [Eq (6)] to fit of the kinetic data:

$$k_d = \frac{k_0 + k_1 K_1^\mathrm{H}[\mathrm{H}^+]}{1 + K_1^\mathrm{H}[\mathrm{H}^+]} \qquad (6)$$

The rate constants of dissociation and the corresponding half-lives calculated in 0.1 M HCl for [Gd**L5**]$^+$ and [Gd**L6**]$^+$ are given in Table 5, which also provides a comparison with different Gd(III) chelates formed with pyclen mono- and dipicolinate chelators, including **L1**-**L4**, as well as with the data published for the corresponding pcta, dota, do2pa and bp12c4 complexes.

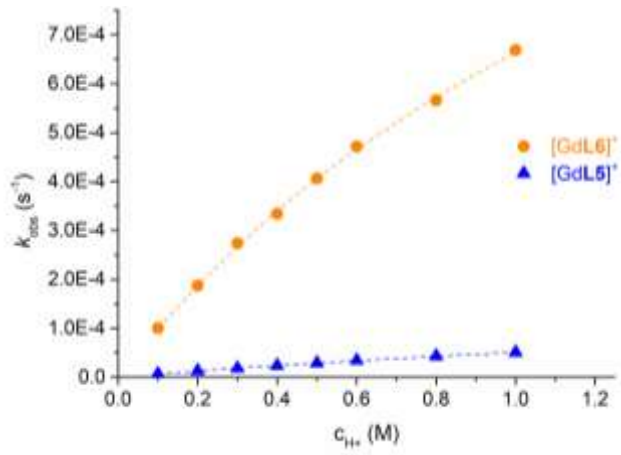

Figure 6. *D*ependence of the pseudo-first-order rate constants (k_{obs}) with proton concentration for the [Gd**L5**]$^+$ (triangles) and [Gd**L6**]$^+$ (circles) complexes ($c_{[GdL5,6]}$ = 1.0 mM). The solid lines correspond to the least-squares fit of the data to equation 6 as described in the text.

The k_1 values confirm the higher inertness of [Gd**L5**]$^+$ compared to [Gd**L6**]$^+$ and also underline the good resistance of [Gd**L5**]$^+$ towards dissociation. Indeed, [Gd**L5**]$^+$ is clearly more inert than both [Gd**L1**] and [Gd**L2**] chelates, and even than the nine-coordinated [Gd**L3**]. The [Gd**L5**]$^+$ complex also surpasses the inertness of [Gd(pcta)]. The structurally related complexes [Gd(do2pa)]$^+$ and [Gd(bp12c4)]$^+$ are rather labile, with the latter having a similar behavior than complexes with open-chain ligands such as dtpa. These results highlight the beneficial effect, in terms of kinetic inertness, of incorporating a rigid pyridine unit into the 12-membered ring of the macrocyclic fragment. The [Gd**L4**] complex remains the most inert among this series of structurally related chelates, with an inertness comparable to that of [Gd(dota)]$^-$.[65]

CONCLUSIONS

The two regioisomers, ligands ***3,9*-pc2pa** (**L5**) or ***3,6*-pc2pa** (**L6**) were synthetized following relevant procedures involving mono-*N*-protected pyclens with Boc and Alloc groups respectively. The synthesis and characterization of the ligands and complexes, including their structural details, photophysical properties, thermodynamic stability and dissociation kinetics are reported in this new study that give new information on the behavior of pyclen-picolinate based ligands. Again, we unambiguously show that it is impossible to predict the properties of Gd^{3+} complexes and that the full control of the synthesis and *N*-functionalization of azamacrocycles is of central importance to highlight new properties and to understand the various mechanisms governing the relaxivity of the complexes.

Here, the symmetrically di-*N*-functionalized pyclen **L5** clearly show attractive properties compared to its dissymmetrical regioisomer **L6** in term of water exchange rate of the Gd(III) complexes that can be explained by the steric hindrance originated by the coordination of the ligand around the water binding site, that favors the dissociatively activated water exchange process. The designed structure is also at the origin of

the high thermodynamic stability of the complex and its relevant inertness.

This study strongly completes the overall knowledge in the chemistry of pyclen-picolinate ligands for lanthanide(III) complexation and gives new information on the various factors governing the water exchange process of the Gd(III) complexes.

EXPERIMENTAL SECTION

Materials and methods. Reagents were purchased from ACROS Organics and from Aldrich Chemical Co and used without further purification. Pyclen·3HCl was provided by Guerbet (Aulnay-sous-bois, France). A solvent purification system was used to dispense dry solvents before each reaction. Pyclen-Boc (**1**)[22] and methyl 6-(chloromethyl)picolinate[14] were synthesized as previously described. Analytical HPLC were performed on a Puriflash Prep C_{18AQ} 5 µM 250× 4.6 mm column with a gradient: 100% H_2O + 0.1% TFA 0→5 min, 0→80% MeOH 5→15 min, 80% MeOH 15→17 min, 80→0% MeOH 17→18min, 100% H_2O + 0.1% TFA 18→20 min; at a flowrate of 1 mL/min and with UV detection at 254 and 350 nm. NMR spectra were recorded at the "Services communs" of the University of Brest. ^{1}H, ^{13}C NMR, DOSY and ^{89}Y-^{1}H HMQC spectra were recorded using Bruker Avance 500 (500 MHz), Bruker Avance 400 (400 MHz), or BrukerAMX 3 300 (300 MHz) spectrometers. HRMS analyses were carried out on a HRMS Q-Tof MaXis instrument equipped with ESI, APCI, APPI and nano-ESI sources (at the Institute of Organic and Analytic Chemistry – ICOA in Orléans).

Synthesis of the ligands

Dimethyl 6,6'-((6-(*tert*-butoxycarbonyl)-3,6,9-triaza-1(2,6)-pyridinacyclodecaphane-3,9-diyl)bis(methylene))dipicolinate (2). A solution of 6-chloromethylpyridine-2-carboxylic acid methylester (2.43 g, 13.1 mmol) and NaI (2.16 g, 14.4 mmol) in dry acetonitrile (110 mL) was added to a solution of Pyclen-boc (**1**) (2.00 g, 6.55 mmol) and K_2CO_3 (1.81 g, 13.1 mmol) in acetonitrile (110 mL). The reaction mixture was stirred at reflux under inert atmosphere for 7 h and the solvent was evaporated. The residue was taken up in dichloromethane and the salts were removed by filtration. The filtrate was concentrated and the crude product was purified by several precipitations by addition of a large excess of Et_2O to the compound dissolved in the minimum amount of MeOH, yielding compound **2** as a yellow oil (3.76 g, 95 %). ^{1}H NMR ($CDCl_3$, 298 K, 300 MHz): δ_H 7.99 (d, ^3J = 6.7 Hz, 2H, ArH picolinate), 7.86 – 7.74 (m, 4H, ArH picolinate), 7.66 (t, ^3J = 7.6 Hz, 1H, ArH pyclen), 7.20 (d, ^2J = 7.6 Hz, 2H, ArH pyclen), 4.06 (s, 4H, CH2 pyclen), 3.97 (s, 6H, OCH_3), 3.92 (d, J = 18.4 Hz, 4H, CH2 picolinate), 3.45 – 3.35 (m, 2H, CH2 pyclen), 3.35 – 3.24 (m, 2H, CH2 pyclen), 2.73 – 2.63 (m, 2H, CH2 pyclen), 2.63 – 2.54 (m, 2H, CH_2 pyclen), 1.17 (s, 9H, CH_3 tert-butyl). ^{13}C NMR ($CDCl_3$, 25°C, 75 MHz): δ_C 165.8 (COOMe), 165.8 (COOMe), 160.7 (C_{quat} picolinate), 160.6 (C_{quat} picolinate), 156.7 (C_{quat} pyclen), 156.4 (C_{quat} pyclen), 155.3 (COO tert-butyl), 147.3 (C_{quat} picolinate), 147.2 (C_{quat} picolinate), 137.5 (CH_{ar} picolinate), 137.4 (CH_{ar} picolinate), 137.3 (CH_{ar} pyclen), 126.0 (CH_{ar} picolinate), 123.7 (CH_{ar} picolinate), 123.0 (CH_{ar} pyclen), 122.8 (CH_{ar} pyclen), 78.9 (C_{quat} tert-butyl), 62.8 (CH_2 picolinate), 62.6 (CH_2 picolinate), 59.9 (CH_2 pyclen), 58.7 (CH_2 pyclen), 52.9 (CH_2 pyclen), 51.5 (CH_2 pyclen), 51.1 (CH_2 pyclen), 45.0 (CH_3 OMe), 44.6 (CH_3 OMe), 28.2 (CH_3 tert-butyl).

6,6'-(3,6,9-Triaza-1(2,6)-pyridinacyclodecaphane-3,9-diylbis(methylene))dipicolinic acid (L5). Compound **2** (156 mg, 0.260 mmol) was dissolved in hydrochloric acid (10.0 mL, 3 M) and the mixture was refluxed overnight. The solvent was evaporated and the crude product was purified by successive precipitations in acetone to yield **L5**·xHCl as an off-white powder (144 mg, 95 %). ^{1}H NMR (D2O, 298 K, 300 MHz): δ_H 8.13 (t, ^3J = 7.9 Hz, 2H), 8.00 (t, ^3J = 7.8 Hz, 1H), 7.92 (d, ^3J = 7.7 Hz, 2H), 7.81 (d, ^3J = 7.9 Hz, 2H), 7.47 (d, ^3J = 7.8 Hz, 2H), 4.72 (s, 4H), 4.56 (s, 4H), 3.55 – 3.43 (m, 4H), 3.38 – 3.19 (m, 4H). ^{13}C NMR (D_2O, 298 K, 75 MHz): δ_H 167.4 (COOH), 155.7 (C_{quat} pyclen), 155.3 (C_{quat} picolinate), 146.6 (C_{quat} picolinate), 145.6 (CH_{ar} picolinate), 144.2 (CH_{ar} pyclen), 131.0 (CH_{ar} picolinate), 128.4 (CH_{ar} picolinate), 126.4 (CH_{ar} pyclen), 61.12 (CH2 picolinate), 61.0 (CH_2 pyclen), 54.59 (CH_2 pyclen), 46.22 (CH_2 pyclen). ESI-HR-MS (positive, H_2O) *m/z* calcd. for $[C_{25}H_{26}FeN_6O_4]^+$, 530.1356; found 530.1359 [M+Fe-2H]+, calcd. for $[C_{25}H_{29}N_6O_4]^+$, 477.2243; found 477.2244 [M+H]+, calcd. for $[C_{25}H_{30}N_6O_4]^{2+}$, 239.1161; found 239.1158 $[M+2H]^{2+}$.

Allyl 9-((6-acetoxypyridin-2-yl)methyl)-6-((6-(methoxycarbonyl)pyridin-2-yl)methyl)-3,6,9-triaza-1(2,6)-pyridinacyclodecaphane-3-carboxylate (4). A solution of compound **3** (702 mg, 2.41 mmol) and K_2CO_3 (1.34 g, 9.67 mmol, 4 equiv) in CH_3CN (60 mL) was stirred at room temperature for 30 min. To this solution was added dropwise a solution of methyl 6-(chloromethyl)picolinate (920 mg, 4.96 mmol, 2.05 equiv) in CH_3CN (57 mL). The reaction mixture was stirred under reflux for 24 h, cooled down to room temperature and salts were filtered off. The filtrate was evaporated to dryness and the residue was taken up in dichloromethane. Residual salts were filtered off and the filtrate was evaporated to dryness. Purification of the residue by column chromatography on alumina (eluent: CH_2Cl_2/MeOH 100/0 to 100/1) gave compound **4** (1.02 g, 1.72 mmol, 71%, mixture of two rotamers) as a yellowish oil. ^{1}H NMR ($CDCl_3$, 298 K, 500 MHz), **the integrations of the signals cannot be measured accurately due to the presence of two rotamers* (1:2 ratio) δ_H 7.97 (m, 5H), 7.90 – 7.72 (m, 8H), 7.64 – 7.52 (m, 5H), 7.48 (m, 5H), 7.28 – 7.23 (m, 5H), 7.12 (m, 4H), 5.88 (ddt, J = 15.9, 10.1, 5.1 Hz, 1H, H25 of the first rotamer), 5.63 (ddt, J = 16.2, 10.7, 5.5 Hz, 2H, H25 of the second rotamer), 5.21 (d, J = 17.2 Hz, 1H, H26a of the first rotamer), 5.14 (d, J = 10.4 Hz, 1H, H26b of the first rotamer), 5.02 (d, J = 17.3 Hz, 1H, H26a of the second rotamer), 4.97 (d, J = 10.5 Hz, 1H, H26b of the second rotamer), 4.59 (s, 6H), 4.54 (d, J = 4.7 Hz, 2H, H24 of the first rotamer), 4.37 (d, J = 5.1 Hz, 4H, H24 of the second rotamer), 3.94 (m, 14H, H22), 3.90 (m, 13H, H22'), 3.80 (m, 7H), 3.73 (s, 4H), 3.68 – 3.60 (m, 6H), 2.69 (br s, 9H), 2.49 (br s, 11H). ^{13}C NMR ($CDCl_3$, 298 K, 126 MHz): mixture of two rotamers δ_C 165.7, 165.6 (C21), 161.1, 160.7 (C16), 157.8, 157.6 (C1, C11), 156.2, 155.9 (C23), 147.2, 147.1 (20), 146.9, 146.8 (?), 137.4, 137.3, 137.2, 136.9 (C13, C18), 132.9, 132.5 (C25), 126.0, 125.4, 123.5, 123.3, 122.7, 122.5, 121.9, 121.5 (Ar), 117.1, 117.0 (C15), 65.9, 65.8 (C24), 61.3, 60.7, 59.5, 54.5 (CH_2), 52.8, 52.7 (C22), 50.6, 50.3, 49.5, 49.1, 48.6, 46.6, 45.7 (CH_2). ESI-HR-MS (positive) *m/z* calcd. for $[C_{31}H_{37}N_6O_6]^+$: 589.2769, found: 589.2762, $[M+H]^+$; calcd.

for $[C_{31}H_{38}N_6O_6]^{2+}$: 295.1421, found: 295.1422, $[M+2H]^{2+}$; 440 = fragmentation.

Methyl 6-((3-((6-acetoxypyridin-2-yl)methyl)-3,6,9-triaza-1(2,6)-pyridinacyclodecaphane-6-yl)methyl)picolinate (5). A solution of compound **4** (100 mg, 0.170 mmol) in CH_2Cl_2 (17 mL) at 0°C was bubbled with N_2 for 45 min and then warmed up to room temperature before addition of $Pd(PPh_3)_4$ (20 mg, 0.02 mmol, 0.1 equiv) and phenylsilane (84 µL, 0.68 mmol, 4 equiv). The reaction mixture was stirred at room temperature for 15 min, concentrated to V=2mL and immediately purified by column chromatography on alumina (eluent: CH_2Cl_2/MeOH/Et_3N 100/0/1 to 100/0.2/1) to give compound **5** (78 mg, 0.15 mmol, 90%) as a white foam. ^{1}H NMR (400 MHz, 298 K, $CDCl_3$): δ_H 7.90 (d, ^3J = 7.6 Hz, 1H, ArH), 7.83 (d, ^3J = 7.6 Hz, 1H, ArH), 7.73 – 7.63 (m, 2H, ArH), 7.59 (t, ^3J = 7.7 Hz, 1H, ArH), 7.45 – 7.34 (m, 2H, ArH), 7.18 (d, ^3J = 7.7 Hz, 1H, ArH), 6.99 (d, ^3J = 7.6 Hz, 1H, ArH), 4.47 (br s, 2H, CH_2 pyclen), 3.97 (s, 3H, OCH_3), 3.94 (s, 3H, OCH_3), 3.88 (s, 2H, CH_2-pico), 3.83 (s, 2H, CH_2-pico), 3.36 (br s, 2H, CH_2 pyclen), 2.88 (br s, 2H, CH_2 pyclen), 2.77 (br s, 4H, CH_2 pyclen). ^{13}C NMR (75 MHz, 298 K, CDCl3): δ_C 165.6, 165.2, 160.2, 158.4, 158.2, 152.0, 147.3, 146.9 (C_q), 137.8, 137.5, 37.1, 126.3, 126.1, 123.7, 123.5, 121.9, 120.9 (Ar), 62.4, 59.6, 57.6, 54.3 (CH_2-pico + CH_2 pyclen), 52.7 (OCH_3), 51.9, 51.6, 50.3 (CH_2 pyclen).

6,6'-(3,6,9-Triaza-1(2,6)-pyridinacyclodecaphane-3,6-diylbis(methylene))dipicolinic acid (L6). A solution of compound **5** (84 mg, 0.17 mmol) in 6 M HCl (2.4 mL) was stirred under reflux for 38 h and then cooled down to room temperature before addition of acetone in large excess. The white precipitate was filtered and dried under vacuum. The filtrate was evaporated to dryness and the residue was purified by a second precipitation (1M HCl/acetone). Both solid were combined to yield 59 mg of **L6**.xHCl as a white solid (60%) ^{1}H NMR (500 MHz, 298 K, D_2O): δ 7.97 – 7.87 (m, 5H), 7.56 (d, ^3J = 7.4 Hz, 1H), 7.51 (t, ^3J = 7.3 Hz, 2H), 7.35 (d, ^3J = 7.7 Hz, 1H), 4.79 (s, 2H under D_2O), 4.58 (br s, 2H), 4.10 (br s, 2H), 3.76 (br s, 2H), 3.47 (br s, 2H), 3.39 – 3.13 (m, 2H), 3.01 (m, 2H). ^{13}C NMR (125 MHz, 298 K, D2O): δ_C 169.9, 169.3, 159.5, 152.7, 152.6, 152.5, 149.5, 149.4 (Cq), 142.9, 142.7, 130.5, 130.1, 128.5, 127.6, 125.3, 124.6 (Ar), 62.1, 61.0 (CH2-pico), 60.0, 56.8, 55.4, 54.6, 53.4, 52.5, 49.5, 48.4 (CH2 pyclen). ESI-HR-MS (positive) *m/z* calcd. for $[C_{25}H_{29}N_6O_4]^+$: 477.2245, found: 477.2235, $[M+H]^+$; calcd. for $[C_{25}H_{30}N_6O_4]^{2+}$: 239.1159, found: 239.1157, $[M+2H]^{2+}$; calcd. for $[C_{25}H_{27}FeN_6O_4]^{2+}$: 265.57160, found: 265.5716, $[M-H+Fe]^{2+}$.

Preparation of the complexes. L.xHCl was dissolved in H_2O (250 µL) and the pH adjusted to 6 with a solution of NaOH 0.1 M. A solution of $MCl_3.6H_2O$ in H_2O (250 µL) was added to the ligand solution and the pH was adjusted again to 6. The mixture was refluxed overnight and then concentrated. The solid was taken up in MeOH and insoluble salts were removed by filtration. The filtrate was concentrated to yield the expected complexes as white solids.

[Gd**L5**]Cl was prepared using **L5**·xHCl (15.0 mg, 0.0260 mmol) and $GdCl_3·6H_2O$ (14.4 mg, 0.0380 mmol) yielding the desired complex as a white powder (16.6 mg, 97 %). ESI-HR-MS (positive, H_2O) *m/z* calcd. for $[C_{25}H_{29}GdN_6O_4]^+$, 632.1251 ; found 632.1251 $[M+H]^+$, calcd. for $[C_{25}H_{28}N_6NaO_4]^+$, 513.2221 ; found 513.2225 [L5+Na]+, calcd. for $[C_{25}H_{30}GdN_6O_4]^{2+}$, 316.5655 ; found 316.5663 $[M+2H]^{2+}$, calcd. for $[C_{25}H_{30}N_6O_4]^{2+}$, 246.1237 ; found 246.1235 [Ligand **L5**+2H]$^{2+}$.

[Y**L5**]Cl was prepared using **L5**·xHCl (15.0 mg, 0.0260 mmol) and $YCl_3·6H_2O$ (11.7 mg, 0.0380 mmol) yielding the desired complex as a white powder (15.1 mg, 99 %). ^{1}H NMR (D_2O, 298 K, 500 MHz): δ_H 8.21 (t, ^3J = 7.6 Hz, 1H), 8.14 (t, ^3J = 7.7 Hz, 1H), 7.99 (d, ^3J = 7.5 Hz, 1H), 7.90 (t, ^3J = 7.6 Hz, 1H), 7.84 (d, ^3J = 7.1 Hz, 1H), 7.82 – 7.77 (m, 2H), 7.48 (d, ^3J = 7.5 Hz, 1H), 7.33 (d, ^3J = 7.6 Hz, 1H), 5.12 (d, ^2J = 15.3 Hz, 1H), 4.84 (d, ^2J = 16.0 Hz, 2H), 4.36 (dd, J = 15.2, 9.5 Hz, 2H), 4.20 (m, 3H), 3.69 – 3.60 (m, 1H), 3.60 – 3.51 (m, 1H), 3.20 – 3.11 (m, 1H), 3.00 (d, ^2J = 12.9 Hz, 1H), 2.85 (d, ^2J = 12.2 Hz, 1H), 2.78 – 2.69 (m, 1H), 2.47 (d, J = 12.8 Hz, 1H), 2.21 – 2.12 (m, 1H), 1.31 – 1.19 (m, 1H). ^{13}C NMR (D2O, 298 K, 125 MHz): δ_C 174.7, 174.7, 161.2, 160.7, 159.8, 159.5, 154.0, 153.5, 145.1, 144.8, 143.7, 129.0, 128.9, 126.2, 126.1, 124.3, 123.4, 65.6, 64.5, 64.3, 63.7, 61.3, 59.7, 58.0, 50.9, 50.7. ^{1}H-^{89}Y HMQC (D_2O, 298 K, 125 MHz: δ_Y 167). ESI-HR-MS (positive, H_2O) *m/z* calcd. for $[C_{25}H_{29}YN_6O_4]^+$, 563.1069 ; found 563.1068 $[M+H]^+$, calcd. for $[C_{25}H_{30}YN_6O_4]^{2+}$, 282.0571; found 282.0570 $[M+2H]^{2+}$.

[Eu**L5**]Cl was prepared using **L5**·xHCl (15.0 mg, 0.0260 mmol) and $EuCl_3·6H_2O$ (14.1 mg, 0.0380 mmol) yielding the desired complex as a white powder (16.6 mg, 95 %). ESI-HR-MS (positive, H_2O) *m/z* calcd. for $[C_{25}H_{29}EuN_6O_4]^+$, 627.1222; found 627.1215 $[M+H]^+$, calcd. for $[C_{25}H_{30}EuN_6O_4]^{2+}$, 314.0661; found 314.0655 $[M+2H]^{2+}$.

[Tb**L5**]Cl was prepared using **L5**·xHCl (15.0 mg, 0.0260 mmol) and $TbCl_3·6H_2O$ (14.3 mg, 0.0380 mmol) yielding the desired complex as a white powder (17.5 mg, 99 %). ESI-HR-MS (positive, H_2O) *m/z* calcd. for $[C_{25}H_{29}TbN_6O_4]^+$, 633.1263 ; found 633.1255 $[M+H]^+$, calcd. for $[C_{25}H_{30}TbN_6O_4]^{2+}$, 317.0674 ; found 317.0668 $[M+2H]^{2+}$.

[Gd**L6**]Cl was prepared using **L6**·xHCl (15.0 mg, 0.0260 mmol) and GdCl3·6H2O (14.4 mg, 0.038 mmol) yielding the desired complex as a white powder (16.7 mg, 98 %). ESI-HR-MS (positive, H_2O) *m/z* calcd. for $[C_{25}H_{29}GdN_6O_4]^+$, 632.1251 ; found 632.1244 $[M+H]^+$, calcd. for $[C_{25}H_{29}N_6NaO_4]^+$, 513.2221 ; found 513.2215 $[M+H]^+$, calcd. for $[C_{25}H_{30}GdN_6O_4]^{2+}$, 316.5655 ; found 316.5661 $[M+2H]^{2+}$, calcd. for $[C_{25}H_{30}N_6O_4]^{2+}$, 246.1237 ; found 246.1233 $[M+2H]^{2+}$.

[Y**L6**]Cl was prepared using **L6**·xHCl (15.0 mg, 0.0260 mmol) and $YCl_3·6H_2O$ (11.7 mg, 0.0380 mmol) yielding the desired complex as a white powder (15.0 mg, 98 %). ^{1}H NMR (D_2O, 298 K, 500 MHz): δ 8.19 (m, 1H), 8.14 (m, 1H), 8.03 (m, 1H), 7.92 (d, J = 7.6 Hz, 1H), 7.84 (t, J = 7.8 Hz, 1H), 7.78 (d, J = 7.6 Hz, 1H), 7.70 (d, J = 7.8 Hz, 1H), 7.42 (d, J = 7.6 Hz, 1H), 7.15 (d, J = 7.8 Hz, 1H), 5.09 (d, J = 17 Hz, 1H), 4.54 (br s, 1H), 4.26 – 4.03 (m, 6H), 3.30 (br s, 1H), 3.02 (d, J = 7.5 Hz, 1H), 2.78 (m, 5H), 2.00 (t, J = 15 Hz, 1H). 13C NMR in D2O, 298 K, 125 MHz: δ 175.0, 175.0, 162.5, 161.7, 161.1, 158.9, 152.8, 145.0, 144.5, 143.4, 129.2, 128.3, 126.7, 126.1, 124.0, 122.5, 66.9, 65.3, 64.7, 62.4, 60.6, 59.0, 52.6. 1H-89Y HMQC NMR in D_2O, 298 K, 125 MHz: δ 148. ESI-HR-MS (positive, H_2O) m/z calcd. for $[C_{25}H_{29}YN_6O_4]$+, 563.1069 ; found 563.1068 $[M+H]^+$, calcd. for $[C_{25}H_{30}YN_6O_4]^{2+}$, 282.0571; found 282.0571 $[M+2H]^{2+}$.

[Eu**L6**]Cl was prepared using **L6**·xHCl (13.9 mg, 0.0240 mmol) and $EuCl_3.6H_2O$ (13.1 mg, 0.0386 mmol) yielding to desired complex as a white powder (13.5 mg, 83 %). ESI-HR-MS (positive, H2O) m/z calcd. for [C25H29EuN6O4]+, 627.1222 ; found 627.1220 $[M+H]^+$, calcd. for $[C25H30EuN6O4]^{2+}$, 314.0661; found 314.0654 $[M+2H]^{2+}$.

[Tb**L6**]Cl was prepared using **L6**·xHCl (13.5 mg, 0.0230 mmol) and $TbCl_3.6H_2O$ (12.7 mg, 0.0340 mmol) yielding to desired complex as a white powder (15.6 mg, quantitative). ESI-HR-MS (positive, H2O) m/z calcd. for [C25H29TbN6O4]+, 633.1263 ; found 633.1257 [M+H]+, calcd. for $[C_{25}H_{30}TbN_6O_4]^{2+}$, 317.0674 ; found 317.0671 $[M+2H]^{2+}$.

Thermodynamic Stability Studies. The protonation constants of the ligands were determined by pH-potentiometric titrations carried out with a Metrohm 888 Titrando titration workstation using a Metrohm-6.0233.100 combined electrode. The titrated solutions (6.00 mL) were thermostated at 25 ºC and the ionic strength in the samples was set to 0.15 M NaCl. The samples were stirred and kept under inert gas atmosphere (N2) to avoid the effect of CO_2. For the pH-calibration of the electrode standard buffers (KH-phthalate, pH=4.005 and borax, pH=9.177) were used. The concentrations of the ligands were determined by pH-potentiometric titrations from the titration data obtained in the presence and absence of large Ca^{2+} excess. In the pH-potentiometric titrations of the ligands 237-303 mL pH data pairs were recorded in the pH range of 1.7-11.9.

The calculation of $[H^+]$ from the measured pH values was performed with the use of the method proposed by Irving *et al.*[66] by titrating a 0.01 M HCl solution (I=0.15 M NaCl) with a standardized NaOH solution. The differences between the measured and calculated pH values were used to obtain the $[H^+]$ concentrations from the pH-data obtained in the titrations. The ion product of water was determined from the same experiment in the pH range 11.2-11.9. Due to the relatively slow formation of the Gd(III) complexes, the so called "out-of-cell" technique was utilized to determine their stability constants. Samples with total volume of 0.50 mL containing $GdCl_3$ (1.00 mM) and the ligand (1.04 mM) were prepared in the acid concentration rage of 0.002 – 0.20 M. The closed samples were kept at 25 ºC for 3 weeks to reach the equilibrium and then the relaxation rates in the samples were measured (the relaxation rates were re-accessed in two weeks in order to ensure that the equilibrium was reached in the samples). The data were fitted by using the concentrations of acid, ligand and metal ion (i.e. ^1H relaxometric method by using the molar relaxivities of the complexes determined independently and as well relaxivities of the samples at the equilibrium). The protonation and stability constants were calculated from the titration data with the PSEQUAD program.[67]

Kinetic Studies. The acid-assisted dissociation of the Gd(III) complexes was studied under pseudo-first order conditions by UV spectrophotometry at 289 nm in thermostated cells (1.0 cm, 25 °C) with a Jasco V770 spectrophotometer in the presence of 1.0 M $(Na^++H^+)Cl^-$. The concentration of the Gd(III) complexes in the samples was set to 0.2 mM. For the calculation of the pseudo-first-order rate constants (k_d), the absorbance values measured at different t times were fitted to Eq (7):

$$A_t = (A_0 - A_e)e^{-k_d t} + A_e \qquad (7)$$

where A_0, A_t and A_e are the absorbance values measured at the start, at time t and at equilibrium, respectively.

Relaxation properties. The ^1H longitudinal (T_1) relaxation times were measured by using Bruker Minispec MQ-20 and MQ-60 NMR Analyzers. The temperature of the sample holder was set 25.0 (±0.2) °C and controlled with a circulating water bath thermostate. The r_{1p} values for the investigated complexes were determined by means of inversion recovery method (180° – τ – 90°) averaging 4-6 data points obtained at 10 different τ delay values. The pH of the 0.3-0.4 mL samples was set to 7.4 in the presence of 0.05 M HEPES buffer.

^{17}O-NMR studies (longitudinal (T_1) and transverse (T_2) relaxation times of the ^{17}O nuclei and chemical shifts) of an aqueous solution of the Gd(III) complex (pH = 7.4, at 18 mM concentration) and of a diamagnetic reference ($HClO_4$ acidified water, pH = 3.0) were measured in the temperature range 273–348 K using a Bruker Avance 400 (9.4 T, 54.2 MHz) spectrometer. The temperature was determined according to well-established calibration routines using ethylene glycol as standard.[68] T_1 and T_2 values were determined by the inversion−recovery and the CPMG techniques, respectively.[69] To avoid susceptibility corrections of the chemical shifts, a glass sphere fitted into a 10 mm NMR tube was used during the measurements. To increase the sensitivity of ^{17}O NMR measurements, ^{17}O enriched water (10% $H_2{}^{17}O$, NUKEM) was added to the solutions to reach a 2% enrichment. The data fit was carried out with the program Micromath Scientist using least squares fitting procedure.

^{17}O NMR data have been fitted according to the Swift and Connick equations.[70] The reduced transverse ^{17}O relaxation rates, $1/T_{2r}$, have been calculated with Eq (8) from the measured relaxation rates $1/T_2$ of the paramagnetic solutions and from the relaxation rates $1/T_{2A}$ of the diamagnetic reference:

$$\frac{1}{T_{2r}} = \frac{1}{P_m}\left[\frac{1}{T_2} - \frac{1}{T_{2A}}\right] = \frac{1}{\tau_m}\frac{T_{2m}^{-2}+\tau_m^{-1}T_{2m}^{-1}+\Delta\omega_m^2}{\left(\tau_m^{-1}+T_{2m}^{-1}\right)^2+\Delta\omega_m^2} \qquad (8)$$

$\Delta\omega_m$ is determined by the hyperfine or scalar coupling constant, $A_O/\hbar$, where B represents the magnetic field, S is the electron spin and g_L is the isotropic Landé g factor [Eq (9)]:

$$\Delta\omega_m = \frac{g_L\mu_B S(S+1)B}{3k_BT}\frac{A_O}{\hbar} \qquad (9)$$

The ^{17}O transverse relaxation rate is mainly determined by the scalar contribution, $1/T_{2sc}$, and is given by Eq(10) and (11):

$$\frac{1}{T_{2m}} \cong \frac{1}{T_{2sc}} = \frac{S(S+1)}{3}\left(\frac{A_O}{\hbar}\right)^2\tau_s \qquad (10)$$

$$\frac{1}{\tau_s} = \frac{1}{\tau_m} + \frac{1}{T_{1e}} \qquad (11)$$

The exchange rate, k_{ex}, (or inverse binding time, τ_m) of the inner sphere water molecule is assumed to obey the Eyring equation [Eq (12)], where $\Delta S^\ddagger$ and $\Delta H^\ddagger$ are the entropy and enthalpy of activation for the exchange, and $k_{ex}{}^{298}$ is the exchange rate at 298.15 K:

$$\frac{1}{\tau_m} = k_{ex} = \frac{k_BT}{h}exp\left\{\frac{\Delta S^\ddagger}{R} - \frac{\Delta H^\ddagger}{RT}\right\} = \frac{k_{ex}^{298}}{298.15}exp\left\{\frac{\Delta H^\ddagger}{R}\left(\frac{1}{298.15} - \frac{1}{T}\right)\right\} \qquad (12)$$

For the fit of the ^{17}O T2 data, we used an exponential function [Eq (13)] to treat the temperature dependency of $1/T_{1e}$:

$$\frac{1}{T_{1e}} = \frac{1}{T_{1e}^{298}}exp\left\{\frac{E_v}{R}\left(\frac{1}{T} - \frac{1}{298.15}\right)\right\} \qquad (13)$$

Crystal structure determination. Single-crystal X-ray diffraction data were collected at 170 K on an X-CALIBUR-2 CCD 4-circle diffractometer (Oxford Diffraction) with graphite monochromatized MoKα radiation (λ = 0.71073). Crystal data and structure refinement details are given in Table S5. Unit-cell determination and data reduction, including interframe scaling, Lorentz, polarization, empirical absorption, and detector sensitivity corrections, were carried out using attached programs of Crysalis software (Oxford Diffraction).[71] Structures were solved by direct methods and refined by the full matrix least-squares method on F^2 with the SHELXL[72] suite of programs. The hydrogen atoms were identified at the last step and refined under geometrical restraints and isotropic U-constraints. Molecular graphics were generated using OLEX2.[73]

Computational details. DFT calculations were carried out with the Gaussian 16 package (Revision B.01).[74] Geometry optimizations and subsequent frequency analysis was carried out with DFT calculations using the M11 exchange correlation functional.[75] The large-core quasirelativistic effective core potential of the Stuttgart/Cologne Group and its associated [5s4p3d]-GTO basis sets was used for Gd,[76] while other atoms were described using the 6-311G(d,p) basis set. Hyperfine coupling constants of the ligand nuclei were obtained using the small-core RECPs of Dolg *et al.* (SCRECP), which includes 28 electrons in the core for Gd, together with the ECP28MWB_GUESS basis set for Gd,[77] and the the EPR-III[78] basis set for the ligand atoms. The effects of bulk water were considered in all calculations using the integral equation formalism of the polarized continuum model (IEFPCM).[79]

ASSOCIATED CONTENT

Supporting Information

The supporting Information including "Coordination polyhedral, ^{1}H, ^{13}C NMR (including 2D) and HRMS spectra, atom numbering of compounds, absorption and emission spectra, cartesian coordinates of $[GdL^6]^{3+}$ obtained with DFT, calculated pseudocontact shifts" is available.

Accession Codes

CCDC 2015848 contains the supplementary crystallographic data for this paper. These data can be obtained free of charge via www.ccdc.cam.ac.uk/data_request/cif, or by emailing data_request@ccdc.cam.ac.uk, or by contacting The Cambridge Crystallographic Data Centre, 12 Union Road, Cambridge CB2 1EZ, UK; fax: + 44 1223 336033.

AUTHOR INFORMATION

Corresponding Authors

*E-mail: raphael.tripier@univ-brest.fr (R. T.)
*E-mail: gyula.tircso@science.unideb.hu (Gy. T.)
*E-mail: Maryline.Beyler@univ-brest.fr (M.B.)

Author Contributions

The manuscript was written through contributions of all authors. All authors have given approval to the final version of the manuscript.

ACKNOWLEDGMENT

R.T. and M.B. acknowledges the Ministère de l'Enseignement Supérieur et de la Recherche and the Centre National de la Recherche Scientifique. R.T. and M.B. also thanks the "Service Commun" of NMR and X-Ray diffraction facilities of the University of Brest. R. T. and O. R. also thank the Guerbet group and the Association Nationale de la Recherche et de la Technologie for the CIFRE fellowship of G.N. C.P.-I. and D. E.-G. acknowledge Centro de Supercomputación de Galicia (CESGA) for providing the computer facilities. The research was funded by the GINOP-2.3.2-15-2016-00008 project supported by the EU and co-supported by the European Regional Development Fund, by the Hungarian National Research, Development and Innovation Office (NKFIH K-120224, 128201 and FK-134551 projects), the bilateral Hungarian-Spanish science and technology cooperation program (2019-2.1.11-TÉT-2019-00084) and the COST Action CA15209 European Network on NMR Relaxometry.

REFERENCES

(1) (a) Parker, D.; Dickins, R. S.; Puschmann, H.; Crossland, C.; Howard, J. A. K. Being Excited by Lanthanide Coordination Complexes: Aqua Species, Chirality, Excited-State Chemistry, and Exchange Dynamics, *Chem. Rev.* **2002**, *102*, 1977-2010; (b) Bonnet, C. S. Zn^{2+} detection by MRI using Ln^{3+}-based complexes: The central role of coordination chemistry. *Coord. Chem. Rev.* **2018**, *369*, 91-104; (c) Amoroso, A. J.; Fallis, I. A.; Pope, S. J. A. Chelating agents for radiolanthanides: Applications to imaging and therapy. *Coord. Chem. Rev.* **2017**, *340*, 198-219.

(2) Wahsner, J.; Gale, E. M.; Rodríguez-Rodríguez, A.; Caravan, P. Chemistry of MRI Contrast Agents: Current Challenges and New Frontiers. Chem. Rev. 2019, 119, 957–1057.

(3) The Chemistry of Contrast Agents in Medical Magnetic Resonance Imaging, Second Edition, 2nd Edn.; Merbach, A., Helm, L., Tóth, É., Eds.; WILEY, 2013.

(4) (a) Heffern, M. C.; Matosziuk, L. M.; Meade, T. J. Lanthanide Probes for Bioresponsive Imaging, *Chem. Rev.* **2014**, *114*, 4496−4539; (b) Bünzli, J.-C. G. Lanthanide Luminescence for Biomedical Analyses and Imaging. *Chem. Rev.* **2010**, *110*, 2729–2755; (c) Bünzli, J.-C. G. On the design of highly luminescent lanthanide complexes. *Coord. Chem. Rev.* **2015**, *293-294*, 19-47; (d) Sy, M.; Nonat, A.; Hildebrandt, N.; Charbonnière, L. J. Lanthanide-based luminescence biolabelling. *Chem. Commun.* **2016**, *52*, 5080-5095.

(5) (a) D' Aléo, A.; Andraud, C.; Maury, O. In Luminescence of Lanthanide Ions in Coordination Compounds and Nanomaterials; De Bettencourt-Diaz, A., Ed.; Wiley, 2014; pp 197−226; (b) Grichine, A.; Haefele, A.; Pascal, S.; Duperray, A.; Michel, R.; Andraud, C.; Maury, O. *Chem. Sci.* **2014**, *5*, 3475-3485.

(6) (a) Charbonniere, L. J. Bringing upconversion down to the molecular scale. *Dalton Trans.* **2018**, *47*, 8566-8570; (b) Nonat, A. M.; Charbonnière, L. J. *Coord. Chem. Rev.* **2020**, *409*, 213192; (c) Golesorkhi, B.; Fürstenberg, A.; Nozary, H.; Piguet, C. Deciphering and quantifying linear light upconversion in molecular erbium complexes. *Chem. Sci.* **2019**, *10*, 6876-6885.

(7) (a) Hu, A.; MacMillan, S. N.; Wilson, J. J. Macrocyclic Ligands with an Unprecedented Size-Selectivity Pattern for the Lanthanide Ions. *J. Am. Chem. Soc.* **2020**, *142*, 13500−13506; (b) Thiele, N. A.; Woods, J. J.; Wilson, J. J. Implementing f-Block Metal Ions in Medicine: Tuning the Size Selectivity of Expanded Macrocycles. *Inorg. Chem.* **2019**, *58*, 10483-10500.

(8) (a) Kostelnik, T. I.; Orvig, C. Radioactive Main Group and Rare Earth Metals for Imaging and Therapy. *Chem. Rev.* **2019**, *119*, 902-956; (b) Hermann, P.; Kotek, J.; Kubícek, V.; Lukes, I. Gadolinium(III) complexes as MRI contrast agents: ligand design and properties of the complexes. *Dalton Trans.* **2008**, 3027–3047; (c) Lukes, I.; Kotek, J.; Vojtisek, P.; Hermann, P. Complexes of tetraazacycles bearing methylphosphinic/phosphonic acid pendant arms with copper(II),

zinc(II) and lanthanides(III). A comparison with their acetic acid analogues. *Coord. Chem. Rev.* **2001**, *216-217*, 287-312; (d) Caravan, P.; Ellison, J. J.; McMurry, T. J.; Lauffer, R. B. Gadolinium(III) Chelates as MRI Contrast Agents: Structure, Dynamics, and Applications. *Chem. Rev.* **1999**, *99*, 2293-2352.

(9) Stasiuk, G. J.; Long, N. The ubiquitous DOTA and its derivatives: the impact of 1,4,7,10-tetraazacyclododecane-1,4,7,10-tetraacetic acid on biomedical imaging. *Chem. Commun.* **2013**, *49*, 2732—2746.

(10) (a) Platas-Iglesias, C.; Mato-Iglesias, M.; Djanashvili, K.; Muller, R. N.; Vander Elst, L.; Peters, J. A.; de Blas, A.; Rodríguez-Blas, T. Lanthanide Chelates Containing Pyridine Units with Potential Application as Contrast Agents in Magnetic Resonance Imaging. *Chem. Eur. J.* **2004**, *10*, 3579-3590; (b) Balogh, E.; Mato-Iglesias, M.; Platas-Iglesias, C.; Tóth, E.; Djanashvili, K.; Peters, J. A.; de Blas, A.; Rodríguez-Blas, T. Pyridine- and Phosphonate-Containing Ligands for Stable Ln Complexation. Extremely Fast Water Exchange on the Gd^{III} Chelates. *Inorg. Chem.* **2006**, *45*, 8719-8728; (c) Mato-Iglesias, M.; Balogh, E.; Platas-Iglesias, C.; Tóth, E.; de Blas, A.; Rodríguez-Blas, T. Pyridine and phosphonate containing ligands for stable lanthanide complexation. An experimental and theoretical study to assess the solution structure. *Dalton Trans.* **2006**, 5404–5415.

(11) Kálmán, F. K.; Végh, A.; Regueiro-Figueroa, M.; Tóth, E.; Platas-Iglesias, C.; Tircsó, G. H4octapa: Highly Stable Complexation of Lanthanide(III) Ions and Copper(II). *Inorg. Chem.* **2015**, *54*, 2345−2356.

(12) Tircsó, G.; Regueiro-Figueroa, M.; Nagy, V.; Garda, Z.; Garai, T.; Kálmán, F. K.; Esteban-Gómez, D.; Tóth, E.; Platas-Iglesias, C. *Chem. Eur. J.* **2016**, *22*, 896 – 901.

(13) (a) Roca-Sabio, A.; Mato-Iglesias, M.; Esteban-Gómez, D.; Tóth, E.; de Blas, A.; Platas-Iglesias, C.; Rodríguez-Blas, T. Macrocyclic Receptor Exhibiting Unprecedented Selectivity for Light Lanthanides. *J. Am. Chem. Soc.* **2009**, *131*, 3331–3341; (b) Roca-Sabio, A.; Mato-Iglesias, M.; Esteban-Gómez, de Blas, A.; Rodríguez-Blas, T.; Platas-Iglesias, C. The effect of ring size variation on the structure and stability of lanthanide(III) complexes with crown ethers containing picolinate pendants. *Dalton Trans.* **2011**, *40*, 384–392.

(14) Mato-Iglesias, M.; Roca-Sabio, A.; Pálinkás, Z.; Esteban-Gómez, D.; Platas-Iglesias, C.; Tóth, É.; de Blas, A.; Teresa Rodríguez-Blas. Lanthanide Complexes Based on a 1,7-Diaza-12-crown-4 Platform Containing Picolinate Pendants: A New Structural Entry for the Design of Magnetic Resonance Imaging Contrast Agents. *Inorg. Chem.* **2008**, *47*, 7840-7851.

(15) Pálinkás, Z.; Roca-Sabio, A.; Mato-Iglesias, M.; Esteban-Gómez, D.; Platas-Iglesias, C.; de Blas, A.; Rodríguez-Blas, T.; Tóth, E. Stability, Water Exchange, and Anion Binding Studies on Lanthanide(III) Complexes with a Macrocyclic Ligand Based on 1,7-Diaza-12-crown-4: Extremely Fast Water Exchange on the Gd^{3+} Complex. *Inorg. Chem.* **2009**, *48*, 8878–8889.

(16) Rodríguez-Rodríguez, A.; Garda, Z.; Ruscsák, E.; Esteban-Gómez, D.; de Blas, A.; Rodríguez-Blas, T.; Lima, L. M. P.; Beyler, M.; Tripier, R.; Tircsó, G.; Platas-Iglesias, C. Stable Mn^{2+}, Cu^{2+} and Ln^{3+} Complexes with Cyclen-Based Ligands Functionalized with Picolinate Pendant Arms. *Dalton Trans.* **2015**, *44*, 5017-5031.

(17) Bui, A. T.; Beyler, M.; Liao, Y.-Y.; Grichine, A.; Duperray, A.; Mulatier, J. C.; Le Guennic, B.; Andraud, C.; Maury, O.; Tripier, R. Cationic Two-Photon Lanthanide Bioprobes Able to Accumulate in Live Cells. *Inorg. Chem.* **2016**, *55*, 7020−7025.

(18) (a) Le Fur, M.; Molnár, E.; Beyler, M.; Fougère, O.; Esteban-Gómez, D.; Rousseaux, O.; Tripier, R.; Tircsó, G.; Platas-Iglesias, C. Expanding the Family of Pyclen-Based Ligands Bearing Pendant Picolinate Arms for Lanthanide Complexation. *Inorg. Chem.* **2018**, *57*, 6932-6945; (b) Le Fur, M.; Beyler, M.; Molnár, E.; Fougère, O.; Esteban-Gómez, D.; Tircsó, G.; Platas-Iglesias, C.; Lepareur, N.; Rousseaux, O.; Tripier, R. The role of the capping bond effect on pyclen $^{nat}Y^{3+}/^{90}Y^{3+}$ chelates: full control of the regiospecific N-functionalization makes the difference. *Chem. Commun.* **2017**, *53*, 9534-9537.

(19) Le Fur, M.; Molnár, E.; Beyler, M.; Kálmán, F. K.; Fougère, O.; Esteban-Gómez, D.; Rousseaux, O.; Tripier, R.; Tircsó, G.; Platas-Iglesias, C. A Coordination Chemistry Approach to Fine-Tune the Physicochemical Parameters of Lanthanide Complexes Relevant to Medical Applications. *Chem. Eur. J.* **2018**, *24*, 3127– 3131.

(20) Nizou, G.; Favaretto, C.; Borgna, F.; Grundler, P. V.; Saffon-Merceron, N.; Platas-Iglesias, C.; Fougère, O.; Rousseaux, O.; van der Meulen, N. P.; Müller, C.; Beyler, M.; Tripier. R. Expanding the Scope of Pyclen-Picolinate Lanthanide Chelates to Potential Theranostic Applications. *Inorg. Chem.* **2020**, *59*, 11736−11748.

(21) Hamon, N.; Roux, A.; Beyler, M.; Mulatier, J.-C.; Andraud, C.; Nguyen, C.; Maynadier, M.; Bettache, N.; Duperray, A.; Grichine, A.; Brasselet, S.; Gary-Bobo, M.; Maury, O.; Tripier, R. Pyclen-Based Ln(III) Complexes as Highly Luminescent Bioprobes for In Vitro and In Vivo One- and Two-Photon Bioimaging Applications. *J. Am. Chem. Soc.* **2020**, *142*, 10184−10197.

(22) Siaugue, J.; Segat-Dioury, F.; Sylvestre, I.; Favre-Réguillon, A.; Foos, J.; Madic, C.; Guy, A. Regioselective Synthesis of N-Functionalized 12-Membered Azapyridinomacrocycles Bearing Trialkylcarboxylic Acid Side Chains. *Tetrahedron* **2001**, *57*, 4713−4718.

(23) Garda, Z.; Molnár, E.; Hamon, N.; Barriada, J. L.; Esteban-Gómez, D.; Váradi. B.;Nagy. V.; Póta, K.; Kálmán, F. K.; Tóth, I.; Lihi, N.; Platas-Iglesias. C.; Tóth, É; Tripier, R.; Tircsó, G. Complexation of Mn(II) by Rigid Pyclen Diacetates: Equilibrium, Kinetic, Relaxometric, DFT and SOD Activity Studies. *Inorg. Chem.* Submitted.

(24) Gao, J.; Ye, K.; He, M.; Xiong, W.-W.; Cao, W.; Lee, Z. Y.; Wang, Y.; Wu, T.; Huo, F.; Liu, X.; Zhang, Q. Tuning Metal–Carboxylate Coordination in Crystalline Metal–Organic Frameworks Through Surfactant Media. *J. Solid State Chem.* **2013**, *206*, 27-31.

(25) (a) Bretonnière, Y.; Mazzanti, M.; Pécaut, J.; Dunand, F. A.; Merbach, A. E. Solid-State and Solution Properties of the Lanthanide Complexes of a New Heptadentate Tripodal Ligand: A Route to Gadolinium Complexes with an Improved Relaxation Efficiency. *Inorg. Chem.* **2001**, *40*, 6737-6745; (b) Bretonnière, Y.; Mazzanti, M.; Pécaut, J.; Dunand, F. A.; Merbach, A. A New Heptadentate Tripodal Ligand Leading to a Gadolinium Complex with an Improved Relaxation Efficiency. *Chem. Commun.* **2001**, 621–622.

(26) Alvarez, S. Polyhedra in (inorganic) chemistry. *Dalton Trans.* **2005**, 2209-2233.

(27) Llunell, M.; Casanova, D.; Cirera, J.; Alemany, P.; Alvarez, S. SHAPE. Program for the Stereochemical Analysis of Molecular Fragments by Means of Continuous Shape Measures and Associated Tools. Version 2.1.

(28) Chatterton, N.; Gateau, C.; Mazzanti, M.; Pécaut, J.; Borel, A.; Helm, L.; Merbach, A. The Effect of Pyridinecarboxylate Chelating Groups on the Stability and Electronic Relaxation of Gadolinium Complexes. *Dalton Trans.* **2005**, 1129-1135.

(29) Liberato, A.; Aguinaco, A.; Clares, M. P.; Delgado-Pinar, E.; Pitarch-Jarque, J.; Blasco, S.; Basallote, M. G.; García-España, E.; Verdejo, B. Pb^{2+} Complexes of Small-Cavity Azamacrocyclic Ligands: Thermodynamic and Kinetic Studies. *Dalton Trans.* **2017**, *46*, 6645–6653.

(30) (a) Kiefer, G. E.; Woods, M. Solid State and Solution Dynamics of Pyridine Based Tetraaza-Macrocyclic Lanthanide Chelates Possessing Phosphonate Ligating Functionality (Ln-PCTMB): Effect on Relaxometry and Optical Properties. *Inorg. Chem.* **2009**, *48*, 11767−11778; (b) Enel, M.; Leygue, N.; Saffon, N.; Galaup, C.; Picard, C. Facile Access to the 12-Membered Macrocyclic Ligand PCTA and Its Derivatives with Carboxylate, Amide, and Phosphinate Ligating Functionalities. *Eur. J. Org. Chem.* **2018**, 1765–1773; (c) Drahos, B.; Kotek, J.; Cisarova, I.; Hermann, P.; Helm, L.; Lukes, I.; Tóth, E. Mn^{2+} Complexes with 12-Membered Pyridine Based Macrocycles Bearing Carboxylate or Phosphonate Pendant Arm: Crystallographic, Thermodynamic, Kinetic, Redox, and $^{1}H/^{17}O$ Relaxation Studies. *Inorg. Chem.* **2011**, *50*, 12785−12801.

(31) Ruiz-Martínez, A.; Alvarez, S. Stereochemistry of Compounds with Coordination Number Ten. *Chem. Eur. J.* **2009**, *15*, 7470–7480.

(32) (a) Price, E. W.; Cawthray, J. F.; Bailey, G. A.; Ferreira, C. L.; Boros, E.; Adam, M. J.; Orvig, C. H_4octapa: An Acyclic Chelator for 111In Radiopharmaceuticals. *J. Am. Chem. Soc.* **2012**, *134*, 8670−8683; (b) Price, E. W.; Zeglis, B. M.; Cawthray, J. F.; Ramogida, C. F.; Ramos, N.; Lewis, J. S.; Adam, M. J.; Orvig, C. H4octapa-Trastuzumab: Versatile Acyclic Chelate System for ^{111}In and ^{177}Lu Imaging and Therapy. *J. Am. Chem. Soc.* **2013**, *135*, 12707−12721.

(33) Edward, J. T. Molecular Volumes and the Stokes-Einstein Equation. *J. Chem. Ed.* **1970**, *47*, 261-270.

(34) Wheate, N. J.; Kumar, P. G. A.; Torres, A. M.; Aldrich-Wright, J. R.; Price, W. S. Examination of Cucurbit[7]uril and Its Host-Guest Complexes by Diffusion Nuclear Magnetic Resonance. *J. Phys. Chem. B* **2008**, *112*, 2311-2314.

(35) (a) Wacker, A.; Carniato, F.; Platas-Iglesias, C.; Esteban-Gomez, D.; Wester, H.-J.; Tei, L.; Notni, J. Dimer Formation of GdDO3A-arylsulfonamide Complexes Causes Loss of pH-Dependency of Relaxivity. *Dalton Trans.* **2017**, **46**, 16828–16836; (b) Roca-Sabio, A.; Bonnet, C. S.; Mato-Iglesias, M.; Esteban-Gómez, D.; Tóth, E.; de Blas, A.; Rodríguez-Blas, T.; Platas-Iglesias, C. Lanthanide Complexes Based on a Diazapyridinophane Platform Containing Picolinate Pendants. *Inorg. Chem.* **2012**, *51*, 10893−10903.

(36) Löble, M. W.; Casimiro, M.; Thielemann, D. T.; Oña-Burgos, P.; Fernández, I.; Roesky, P. W.; Breher. F. ^{1}H,^{89}Y HMQC and Further NMR Spectroscopic and X-ray Diffraction Investigations on Yttrium-Containing Complexes Exhibiting Various Nuclearities. *Chem. Eur. J.* **2012**, *18*, 5325–5334.

(37) Miéville, P.; Jannin, S.; Helm, L.; Bodenhausen, G. Kinetics of Yttrium-Ligand Complexation Monitored Using Hyperpolarized ^{89}Y as a Model for Gadolinium in Contrast Agents. *J. Am. Chem. Soc.* **2010**, *132*, 5006–5007.

(38) Xing, Y.; Jindal, A. K.; Regueiro-Figueroa, M.; Le Fur, M.; Kervarec, N.; Zhao, P.; Kovacs, Z.; Valencia, L.; Pérez-Lourido, P.; Tripier, R.; Esteban-Gómez, D.; Platas-Iglesias, C.; Sherry, A. D. The Relationship between NMR Chemical Shifts of Thermally Polarized and Hyperpolarized ^{89}Y Complexes and Their Solution Structures. Chem. Eur. J. 2016, 22, 16657–16667.

(39) Le Fur, M.; Beyler, M.; Molnár, E.; Fougère, O.; Esteban-Gómez, D.; Tircsó, G.; Platas-Iglesias, C.; Lepareur, N.; Rousseaux, O.; Tripier, R. Stable and Inert Yttrium(III) Complexes with Pyclen-Based Ligands Bearing Pendant Picolinate Arms: Toward New Pharmaceuticals for β-Radiotherapy. *Inorg. Chem.* **2018**, *57*, 2051−2063.

(40) Sy, M.; Esteban-Gómez, D.; Platas-Iglesias, C.; Rodríguez-Rodríguez, A.; Tripier, R.; Charbonnière, L. J. Spectroscopic Properties of a Family of Mono- to Trinuclear Lanthanide Complexes. *Eur. J. Inorg. Chem.* **2017**, 2122–2129.

(41) (a) Nocton, G.; Nonat, A.; Gateau, C.; Mazzanti, M. Water Stability and Luminescence of Lanthanide Complexes of Tripodal Ligands Derived from 1,4,7-Triazacyclononane: Pyridinecarboxamide versus Pyridinecarboxylate Donors. *Helv. Chim. Acta* **2009**, *92*, 2257-2273; (b) Guanci, C.; Giovenzana, G.; Lattuada, L.; Platas-Iglesias, C.; Charbonnière, L. J. AMPED: A New Platform for Picolinate Based Luminescent Lanthanide Chelates. *Dalton Trans.* **2015**, *44*, 7654–7661.

(42) Beeby, A.; Clarkson, I. M.; Dickins, R. S.; Faulkner, S.; Parker, D.; Royle, L.; de Sousa, A. S.; Williams, J. A. G.; Woods, M. Non-Radiative Deactivation of the Excited States of Europium, Terbium and Ytterbium Complexes by Proximate Energy-Matched OH, NH and CH Oscillators: An Improved Luminescence Method for Establishing Solution Hydration States. *J. Chem. Soc., Perkin Trans. 2* **1999**, 493–503.

(43) Chauvin, A.-S.; Gumy, F.; Imbert, D.; Bünzli, J.-C. G. Europium and Terbium tris(Dipicolinates) as Secondary Standards for Quantum Yield Determination. *Spectrosc. Lett.* **2004**, *37*, 517-532 (erratum *Spectrosc. Lett.* **2007**, *40*, 193).

(44) (a) Nonat, A.; Giraud, M.; Gateau,C.; Fries, P. H.; Helm, L.; Mazzanti, M. Gadolinium(III) Complexes of 1,4,7-Triazacyclononane Based Picolinate Ligands: Simultaneous Optimization of Water Exchange Kinetics and Electronic Relaxation. *Dalton Trans.* **2009**, 8033–8046; (b) Nonat, A.; Gateau, C.; Fries, P. H.; Mazzanti, M. Lanthanide Complexes of a Picolinate Ligand Derived from 1,4,7-Triazacyclononane with Potential Application in Magnetic Resonance Imaging and Time-Resolved Luminescence Imaging. *Chem. Eur. J.* **2006**, *12*, 7133 – 7150.

(45) Binnemans, K. Interpretation of Europium(III) Spectra. *Coord. Chem. Rev.* **2005**, *295*, 1-45.

(46) Werts, M. H. V.; Jukes, R. T. F.; Verhoeven, J. W. The Emission Spectrum and the Radiative Lifetime of Eu^{3+} in Luminescent Lanthanide Complexes. *Phys. Chem. Chem. Phys.* **2002**, *4*, 1542–1548.

(47) Bruce, J. I.; Dickins, R. S.; Govenlock, l. J.; Gunnlaugsson, T.; Lopinski, S.; Lowe, M. P.; Parker, D.; Peacock, R. D.; Perry, J. J. B.; Aime, S.; Botta, M. The Selectivity of Reversible Oxy-Anion Binding in Aqueous Solution at a Chiral Europium and Terbium Center: Signaling of Carbonate Chelation by Changes in the Form and Circular Polarization of Luminescence Emission. *J. Am. Chem. Soc.* **2000**, *122*, 9674-9684.

(48) Caravan, P.; Esteban-Gómez, D.; Rodríguez-Rodríguez, A.; Platas-Iglesias, C. Water exchange in lanthanide complexes for MRI applications. Lessons learned over the last 25 years. *Dalton Trans.* **2019**, *48*, 11161–11180.

(49) Micskei, K.; Powell, D. H.; Helm, L.; Brücher, E.; Merbach, A. E. Water Exchange on $[Gd(H_2O)J^{3+}$ and $[Gd(PDTA)(H_2O)_2]^-$ in Aqueous Solution: a Variable-Pressure, -Temperature and –Magnetic Field ^{17}O NMR Study. *Magn. Reson. Chem.* **1993**, *31*, 1011-1020.

(50) Aime, S.; Barge, A.; Bruce, J. I.; Botta, M.; Howard, J. A. K.; Moloney, J. M.; Parker, D.; de Sousa, A. S.; Woods, M. NMR, Relaxometric, and Structural Studies of the Hydration and Exchange Dynamics of Cationic Lanthanide Complexes of Macrocyclic Tetraamide Ligands. *J. Am. Chem. Soc.* **1999**, *121*, 5762-5771.

(51) Lammers, H.; Maton, F.; Pubanz, D.; van Laren, M. W.; van Bekkum, H.;. Merbach, A. E.; Muller, R. N.; Peters, J. A.. Structures and Dynamics of Lanthanide(III) Complexes of Sugar-Based DTPA-bis(amides) in Aqueous Solution: A Multinuclear NMR Study. *Inorg. Chem.* **1997**, *36*, 2527-2538.

(52) (a) Esteban-Gomez, D.; de Blas, A.; Rodriguez-Blas, T.; Helm, L.; Platas-Iglesias, C. Hyperfine Coupling Constants on Inner-Sphere Water Molecules of Gd^{III}-Based MRI Contrast Agents. *ChemPhysChem* **2012**, *13*, 3640-3650; (b) Regueiro-Figueroa, M.; Platas-Iglesias, C. Toward the Prediction of Water Exchange Rates in Magnetic Resonance Imaging Contrast Agents: A Density Functional Theory Study. *J. Phys. Chem. A* **2015**, *119*, 6436−6445.

(53) Powell, D. H.; Ni Dhubhghaill, O. M.; Pubanz, D.; Helm, L.; Lebedev, Y. S.; Schlaepfer, W.; Merbach, A. E. Structural and Dynamic Parameters Obtained from ^{17}O NMR, EPR, and NMRD Studies of Monomeric and Dimeric Gd^{3+} Complexes of Interest in Magnetic Resonance Imaging: An Integrated and Theoretically Self-Consistent Approach *J. Am. Chem. Soc.* **1996**, **118**, 9333-9346.

(54) Aime, S.; Botta, M.; Geninatti Crich, S.; Giovenzana, G.; Pagliarin, R.; Sisti, M.; Terreno, E. NMR relaxometric studies of Gd(III) complexes with heptadentate macrocyclic ligands. *Magn. Reson. Chem.* **1998**, *36*, S200-S208.

(55) Borel, A.; Laus, S.; Ozarowski, A.; Gateau, C.; Nonat, A.; Mazzanti, M.; Helm, L. Multiple-Frequency EPR Spectra of Two Aqueous Gd^{3+} Polyamino Polypyridine Carboxylate Complexes: A Study of High Field Effects. *J. Phys. Chem. A* **2007**, *111*, 5399-5407.

(56) Borel, A.; Kang, H.; Gateau, C.; Mazzanti, M.; Clarkson, R. B.; Belford, R. L. Variable Temperature and EPR Frequency Study of Two Aqueous Gd(III) Complexes with Unprecedented Sharp Lines. *J. Phys. Chem. A* **2006**, *110*, 12434-12438.

(57) (a) Rodríguez-Rodríguez, A.; Regueiro-Figueroa, M.; Esteban-Gómez, D.; Rodríguez-Blas, T.; Patinec, V.; Tripier, T.; Tircsó, G.; Carniato, F.; Botta, M.; Platas-Iglesias, C. Definition of the Labile Capping Bond Effect in Lanthanide Complexes. *Chem. Eur. J.* **2017**, *23*, 1110 – 1117; (b) Garda, Z.; Nagy, V.; Rodríguez-Rodríguez, A.; Pujales-Paradela, R.; Patinec, V.; Angelovski, G.; Tóth, E.; Kálmán, F. K.; Esteban-Gómez, D.; Tripier, R.; Platas-Iglesias, C.; Tircsó, G. Unexpected Trends in the Stability and Dissociation Kinetics

of Lanthanide(III) Complexes with Cyclen-Based Ligands across the Lanthanide Series. *Inorg. Chem.* **2020**, *59*, 8184−8195.

(58) Boros, E.; Polasek, M.; Zhang, Z.; Caravan, P. Gd(DO-TAla): A Single Amino Acid Gd-complex as a Modular Tool for High Relaxivity MR Contrast Agent Development. *J. Am. Chem. Soc.* **2012**, *134*, 19858−19868.

(59) Aime, S.; Botta, M.; Geninatti-Crich, S.; Giovenzana, G. B.; Jommi, G.; Pagliarin, R.; Sisti, M. Synthesis and NMR Studies of Three Pyridine-Containing Triaza Macrocyclic Triacetate Ligands and Their Complexes with Lanthanide Ions. *Inorg. Chem.* **1997**, *36*, 2992-3000.

(60) Ferreirós-Martínez, R.; Esteban-Gómez, D.; de Blas, A.; Platas-Iglesias, C.; Rodríguez-Blas, T. Eight-Coordinate Zn(II), Cd(II), and Pb(II) Complexes Based on a 1,7-Diaza-12-crown-4 Platform Endowed with a Remarkable Selectivity over Ca(II). *Inorg. Chem.* **2009**, *48*, 11821–11831.

(61) Regueiro-Figueroa, M.; Bensenane, B.; Ruscsák, E.; Esteban-Gomez, D.; Charbonnière, L. J.; Tircsó, G.; Tóth, I.; de Blas, A.; Rodríguez-Blas, T.; Platas-Iglesias, C. Lanthanide dota-like Complexes Containing a Picolinate Pendant: Structural Entry for the Design of Ln^{III}-Based Luminescent Probes. *Inorg. Chem.* **2011**, *50*, 4125–4141.

(62) Burai, L.; Fábián, I.; Király, R.; Szilágyi, E.; Brücher, E. Equilibrium and Kinetic Studies on the Formation of the Lanthanide(III) Complexes, $[Ce(dota)]^-$ and $[Yb(dota)]^-$ (H_4dota = 1,4,7,10-tetraazacyclododecane-1,4,7,10-tetraacetic acid). *J. Chem. Soc., Dalton Trans.* **1998**, 243-248.

(63) Xu, J.; Franklin, S. J.; Whisenhunt, D. W.; Raymond, K. N. Gadolinium Complex of Tris[(3-hydroxy-l-methyl-2-oxo-l,2-didehydropyridine-4-carboxamido)ethyl]-amine: A New Class of Gadolinium Magnetic Resonance Relaxation Agents. *J. Am. Chem. Soc.* **1995**, *117*, 7245–7246.

(64) Baranyai, Z.; Pálinkás, Z.; Uggeri, F.; Maiocchi, A.; Aime, S.; Brücher, E. Dissociation Kinetics of Open-Chain and Macrocyclic Gadolinium(III)-Aminopolycarboxylate Complexes Related to Magnetic Resonance Imaging: Catalytic Effect of Endogenous Ligands. *Chem. - Eur.* J. **2012**, *18*, 16426-16435.

(65) Wedeking, P.; Kumar, K.; Tweedle, M. F. Dissociation of gadolinium chelates in mice: Relationship to chemical characteristics. *Magn. Reson. Imaging* **1992**, *10*, 641-648.

(66) Irving, H. M.; Miles, M. G.; Pettit, L. D. A Study of Some Problems in Determining the Stoicheiometric Proton Dissociation Constants of Complexes by Potentiometric Titrations Using A Glass Electrode. *Anal. Chim. Acta* **1967**, *38*, 475-488.

(67) Zekany L., Nagypal I. PSEQUAD, in Computational Methods for the Determination of Formation Constants. Modern Inorganic Chemistry. Leggett D. J. (Ed), Springer, Boston, 1985.

(68) Raiford, D. S.; Fisk, C. L.; Becker, E. D. Calibration of Methanol and Ethylene Glycol Nuclear Magnetic Resonance Thermometers. *Anal. Chem.* **1979**, *51*, 2050-2051.

(69) (a) Carr, H. Y.; Purcell, E. M. Effects of Diffusion on Free Precession in Nuclear Magnetic Resonance Experiments. *Phys. Rev.* **1954**, *94*, 630-638. (b) Meiboom, S.; Gill, D., Modified Spin-Echo Method for Measuring Nuclear Relaxation Times. *Rev. Sci. Instrum.* **1958**, *29*, 688-691.

(70) (a) Swift, T. J.; Connick, R. E. NMR-Relaxation Mechanisms of O^{17} in Aqueous Solutions of Paramagnetic Cations and the Lifetime of Water Molecules in the First Coordination Sphere. *J. Chem. Phys.* **1962**, *37*, 307−320. (b) Swift, T. J.; Connick, R. E. NMR-Relaxation Mechanisms of ^{17}O in Aqueous Solutions of Paramagnetic Cations and the Lifetime of Water Molecules in the First Coordination Sphere. *J. Chem. Phys.* **1964**, *41*, 2553.

(71) *Crysalis Software System*, version 1.171.28 cycle4 beta; Oxford Diffraction Ltd.: Abingdon, U.K, 2005.

(72) Sheldrick, G. M. A Short History of SHELX. *Acta Crystallogr., Sect. A: Found. Crystallogr.* **2008**, *64*, 112−122.

(73) Dolomanov, O. V.; Bourhis, L. J.; Gildea, R. J.; Howard, J. A.. K.; Puschmann, H. OLEX: A Complete Structure Solution, Refinement and Analysis Program. *J. Appl. Cryst.* **2009**, *42*, 339-341.

(74) Gaussian 16, Revision B.01, Frisch, M. J.; Trucks, G. W.; Schlegel, H. B.; Scuseria, G. E.; Robb, M. A.; Cheeseman, J. R.; Scalmani, G.; Barone, V.; Petersson, G. A.; Nakatsuji, H.; Li, X.; Caricato, M.; Marenich, A. V.; Bloino, J.; Janesko, B. G.; Gomperts, R.; Mennucci, B.; Hratchian, H. P.; Ortiz, J. V.; Izmaylov, A. F.; Sonnenberg, J. L.; Williams-Young, D.; Ding, F.; Lipparini, F.; Egidi, F.; Goings, J.; Peng, B.; Petrone, A.; Henderson, T.; Ranasinghe, D.; Zakrzewski, V. G.; Gao, J.; Rega, N.; Zheng, G.; Liang, W.; Hada, M.; Ehara, M.; Toyota, K.; Fukuda, R.; Hasegawa, J.; Ishida, M.; Nakajima, T.; Honda, Y.; Kitao, O.; Nakai, H.; Vreven, T.; Throssell, K.; Montgomery, J. A., Jr.; Peralta, J. E.; Ogliaro, F.; Bearpark, M. J.; Heyd, J. J.; Brothers, E. N.; Kudin, K. N.; Staroverov, V. N.; Keith, T. A.; Kobayashi, R.; Normand, J.; Raghavachari, K.; Rendell, A. P.; Burant, J. C.; Iyengar, S. S.; Tomasi, J.; Cossi, M.; Millam, J. M.; Klene, M.; Adamo, C.; Cammi, R.; Ochterski, J. W.; Martin, R. L.; Morokuma, K.; Farkas, O.; Foresman, J. B.; Fox, D. J. Gaussian, Inc., Wallingford CT, 2016.

(75) Peverati, R.; Truhlar, D. G. Improving the Accuracy of Hybrid Meta-GGA Density Functionals by Range Separation. *J. Phys. Chem. Lett.* **2011**, *2*, 2810-2817.

(76) Dolg, M.; Stoll, H.; Savin, A.; Preuss, H. Energy-adjusted pseudopotentials for the rare earth elements. *Theor. Chim. Acta* **1989**, *75*, 173-194.

(77) Dolg, M.; Stoll, H.; Preuss, H. Energy-adjusted Ab Initio Pseudopotentials for the Rare Earth Elements. *J. Chem. Phys.* **1989**, *90*, 1730−1734.

(78) Rega, N.; Cossi, M.; Barone, V. Development and Validation of Reliable Quantum Mechanical Approaches for the Study of Free Radicals in Solution. *J. Chem. Phys.* **1996**, *105*, 11060−11067.

(79) Tomasi, J.; Mennucci, B.; Cammi, R. Quantum Mechanical Continuum Solvation Models. *Chem. Rev.* **2005**, *105*, 2999-3093.